

Fusion Reactor Technology 2

(459.761, 3 Credits)

Prof. Dr. Yong-Su Na

(32-206, Tel. 880-7204)

Stability

- **Energy Principle**

$$\omega^2 = \frac{\delta W}{K} \geq 0 \quad \text{stable}$$

$$\delta W \geq 0 \quad \text{stable}$$

$$\delta W = \delta W_F + \delta W_S + \delta W_V$$

$$\delta W_F = \frac{1}{2} \int_V dr \left[\frac{|\vec{Q}|^2}{\mu_0} - \vec{\xi}_\perp^* \cdot (\vec{J} \times \vec{Q}) + \gamma p |\nabla \cdot \vec{\xi}|^2 + (\vec{\xi}_\perp \cdot \nabla p) \nabla \cdot \vec{\xi}_\perp^* \right]$$

$$\delta W_S = \frac{1}{2} \int_S dS |\vec{n} \cdot \vec{\xi}_\perp|^2 \vec{n} \cdot [(\nabla(p + B^2 / 2\mu_0))]$$

$$\delta W_V = \frac{1}{2} \int_V dr \frac{|\hat{B}_1|^2}{\mu_0}$$

$\vec{\xi}$: displacement of the plasma

away from its equilibrium position

$$\vec{Q} \equiv \hat{B}_1 = \nabla \times (\vec{\xi} \times \vec{B})$$

Boundary conditions on trial functions

$$\vec{n} \cdot \hat{B}_1|_{r_w} = 0 \quad \vec{n} \cdot \hat{B}_1|_{r_p} = \hat{B}_1 \cdot \nabla (\vec{n} \cdot \vec{\xi}_\perp) - (\vec{n} \cdot \vec{\xi}_\perp) [\vec{n} \cdot (\vec{n} \cdot \nabla) \hat{B}_1]|_{r_p}$$

Stability

- The Intuitive Form of δW_F

$$\delta W_F = \frac{1}{2} \int_V dr \left[\frac{|\vec{Q}_\perp|^2}{\mu_0} + \frac{B^2}{\mu_0} |\nabla \cdot \vec{\xi}_\perp + 2\vec{\xi}_\perp \cdot \vec{\kappa}|^2 + \gamma p |\nabla \cdot \vec{\xi}|^2 - 2(\vec{\xi}_\perp \cdot \nabla p)(\vec{\kappa} \cdot \vec{\xi}_\perp^*) - J_\parallel (\vec{\xi}_\perp^* \times \vec{b}) \cdot \vec{Q}_\perp \right]$$

↓
↓
↓
↓
↓
↓
↓

Energy required to bend magnetic field lines: dominant potential energy contribution to the shear Alfvén wave
Energy necessary to compress the magnetic field: major potential energy contribution to the compressional Alfvén wave
Energy required to compress the plasma: main source of potential energy for the sound wave

Tokamak Stability

- Considering plasma states which are not in perfect thermodynamic equilibrium (no exact Maxwellian distribution, e.g. non-uniform density), even though they represent equilibrium states in the sense that the force balance is equal to 0 and a stationary solution exists, means their entropy is not at the maximum possible and hence free energy appears available which can excite perturbations to grow:
unstable equilibrium state
- The gradients of plasma current magnitude and pressure are the destabilising forces in connection with the bad magnetic field curvature

Tokamak Instabilities

- **Macroscopic MHD instabilities**

- **Ideal MHD instabilities**

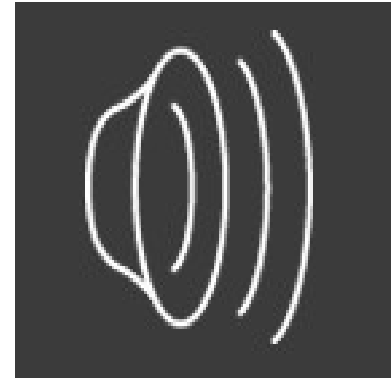
- current driven (kink) instabilities
 - internal modes
 - external modes
- pressure driven instabilities
 - interchange modes
 - ballooning modes
- current+pressure driven: edge localised modes (ELMs)
- vertical instability

At high pressure, the two origins of instabilities, current and pressure start to interact with each other

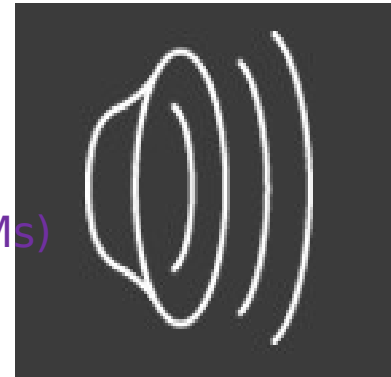
- **Resistive MHD instabilities**

- current driven instabilities
 - tearing modes
 - neoclassical tearing modes (NTMs)

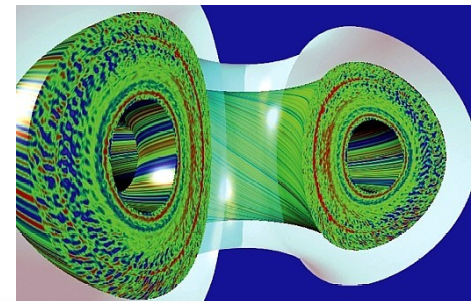
- **Microinstabilities - Transport**



Flux conservation
Topology unchanged



Reconnection of field lines
Topology changed



Classification of MHD Instabilities

- **Internal/Fixed Boundary Modes** $n \cdot \xi \Big|_{S_p} = 0$
 - Mode structure does not require any motion of the plasma-vacuum interface away from its equilibrium position
 - Singular surface ($\mathbf{B} \cdot \nabla = 0$) inside the plasma
 - δW_F only needed to be considered ($\delta W_S = \delta W_V = 0$)
- **External/Free-Boundary Modes** $n \cdot \xi \Big|_{S_p} \neq 0$
 - plasma-vacuum interface moving from its equilibrium position during an unstable MHD perturbation
 - Singular surface in the vacuum region

Classification of MHD Instabilities

- **Current-Driven Modes**

- Driven by parallel currents and can exist even with $\nabla p = 0$
- Often known as “kink” modes
- The most unstable one: Internal modes with long parallel wavelengths and macroscopic perpendicular wavelengths $k_{\perp} a \sim 1$

- **Pressure-Driven Modes**

- Driven by perpendicular currents
- The most unstable one: Internal modes with very short wavelengths perpendicular to the magnetic field but long wavelengths parallel to the field

Stability

- **MHD modes**

- Normal modes of perturbation of 'straightened out' torus (standing wave)

$$\xi = \xi_0 e^{i[(k_\theta l_\theta + k_\phi l_\phi) - \omega t]} = \xi_0 e^{i\left(\frac{m}{r} r\theta - \frac{n}{R} R\phi\right)} e^{\gamma t} = \xi_0 e^{i(m\theta - n\phi)} e^{\gamma t}$$

Periodic boundary conditions:

$$k_\theta = \frac{2\pi}{\lambda_\theta} = \frac{m}{r}, \quad k_\phi = \frac{2\pi}{\lambda_\phi} = -\frac{n}{R}$$

$$\Leftrightarrow 2\pi r = m\lambda_\theta, \quad 2\pi R = -n\lambda_\phi$$

ξ : displacement of the plasma away from its equilibrium position

m, n : poloidal, toroidal mode number

γ : growth rate

negative sign simply for convenience

- Resonance surface: magnetic line pitch coincides with the helical perturbation pitch

$$\vec{k} \cdot \vec{B} \equiv \frac{mB_\theta}{r} - \frac{nB_\phi}{R} = \frac{B_\theta}{r} (m - nq(r)) = 0 \Rightarrow q(r) \equiv \frac{rB_\phi}{RB_\theta(r)} = \frac{m}{n}$$

HW: why $\vec{k} \cdot \vec{B} = 0$ when the perturbation can be resonant?

Ideal MHD Instabilities

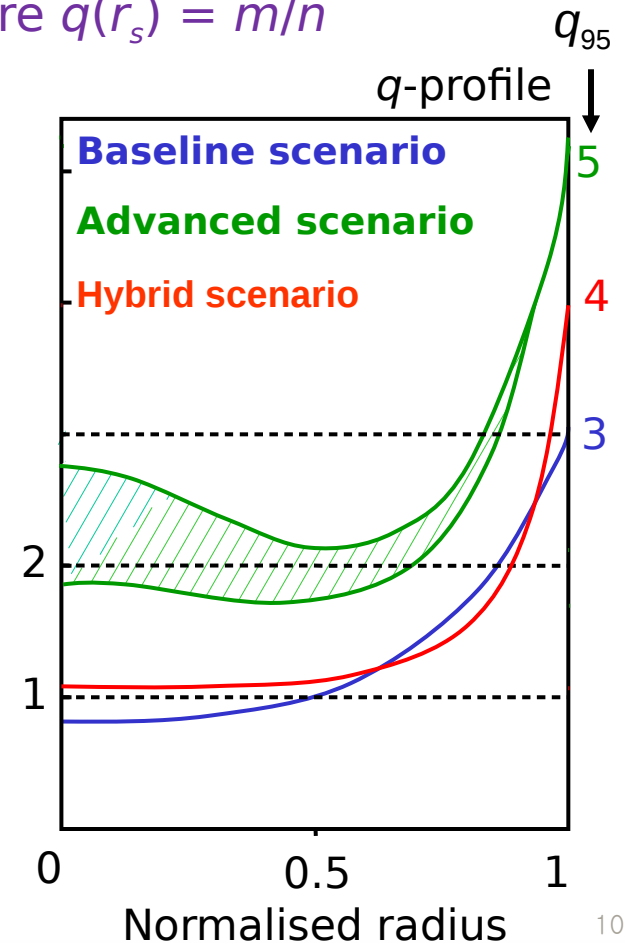
- **The most Virulent Instabilities**
 - fast growth (microseconds)
 - the possible extension over the entire plasma

Ideal MHD Instabilities

- **Internal Kink Modes**

- fixed boundary modes
- localised near rational surface $r = r_s$ where $q(r_s) = m/n$
($\mathbf{k} \cdot \mathbf{B} = 0$ for resonance)
- stability condition for $m = 1, n = 1$ mode

$$q_0 > 1$$



Ideal MHD Instabilities

- **External Kink Modes**

- free surface modes

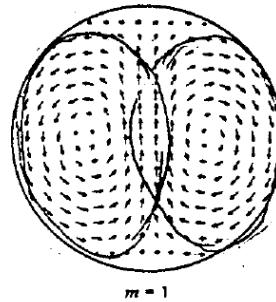
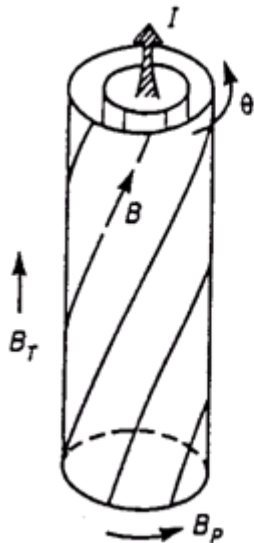
- ($m = 0$ sausage, $m = 1$ helical kink, $m = 2, 3, \dots$ surface kinks)

- localised near rational surface $r = r_s$ where $q(r_s) = m/n$

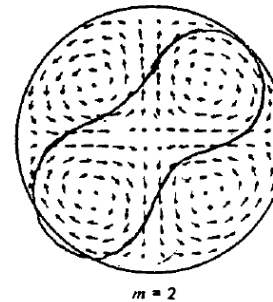
- (m, n) modes fall on plasma surface $r = a$ (vacuum region):

- mode rational surface $q(a) = m/n$

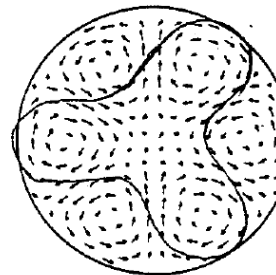
- fastest and most dangerous



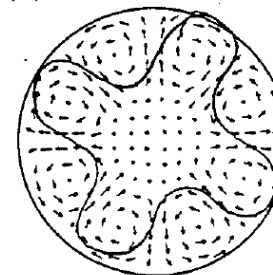
$m = 1$



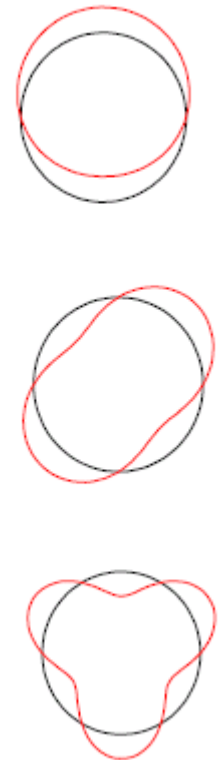
$m = 2$



$m = 3$



$m = 4$



Ideal MHD Instabilities

- **External Kink Modes**
 - **Stabilising effects and stability conditions**
 - conducting wall stabilisation for low n modes
 - strong toroidal magnetic field
 - $q(a) > m/n$ for (m, n) modes w/o conducting wall
- Kruskal-Shafranov limit for $m = n = 1$ mode

Ideal MHD Instabilities

- $m = n = 1$ external kink mode: Kruskal-Shafranov limit

In the limit where the conducting wall moves to infinity

$$\frac{\delta W_2}{W_0} = \xi_0^2 \left(n - \frac{1}{q_a} \right) \left[\left(n - \frac{1}{q_a} \right) + \left(n + \frac{1}{q_a} \right) \right] = 2\xi_0^2 \left[n \left(n - \frac{1}{q_a} \right) \right]$$

$q_a > 1$ Kruskal-Shafranov criterion:
stability condition for the $m = 1$ external kink mode
for the worst case, $n = 1$

Imposing an important constraint on tokamak operation:
toroidal current upper limit ($I < I_{KS}$)

$$I_{KS} \equiv 2\pi a^2 B_\phi(R_0) / \mu_0 R_0 = 5a^2 B_\phi(R_0) / R_0 \text{ [MA]}$$

$$q_a = \frac{aB_\phi(R_0)}{R_0 B_p} = \frac{aB_\phi(R_0)}{R_0 \mu_0 I_{KS} / 2\pi a} = 1$$

Ideal MHD Instabilities

- **External Kink Modes**
 - **Stabilising effects and stability conditions**

- conducting wall stabilisation for low n modes
- strong toroidal magnetic field
- $q(a) > m/n$ for (m, n) modes w/o conducting wall

Kruskal-Shafranov limit for $m = n = 1$ mode

- centrally peaked toroidal current density profile for $m \geq 2$

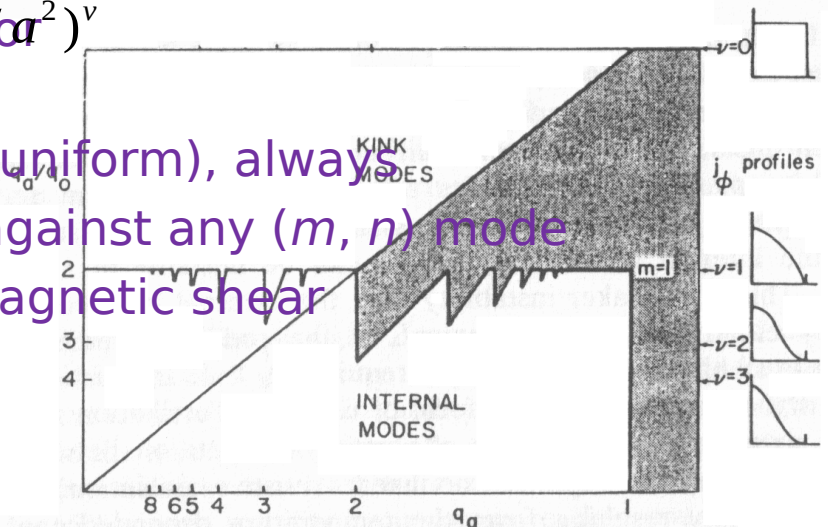
$$\frac{q_a}{q_0} \geq \nu + 1 \approx 2 - 3$$

$$J_\phi = J_0 (1 - r^2/a^2)^\nu$$

for $\nu = 0$ (uniform), always unstable against any (m, n) mode

- strong magnetic shear

$$s(r) \equiv \frac{r}{q} \frac{dq}{dr}$$



Ideal MHD Instabilities

- **Interchange Modes**

- Interchange perturbations do not grow in normal tokamaks if $q \geq 1$.
- locally grow in the outboard bad curvature region: ballooning modes
- internal modes: localised near rational surface $r = r_s$ where
$$q(r_s) = m/n$$
- no threat to confinement unless $q(0) \ll 1$

- **Interchange Modes**

- **Stabilising effects and stability conditions**

- minimum- B configuration
- magnetic shear
- Mercier necessary condition
- elongated outward triangular cross section

Ideal MHD Instabilities

- Internal localised interchange instabilities: Mercier criterion

$$\frac{d}{dx} \left(x^2 \frac{d\xi}{dx} \right) + D_s \xi = 0 \quad \begin{array}{l} \text{Straight tokamak:} \\ \text{Euler-Lagrange equation} \end{array}$$

$$\xi = x^p$$

$$p(p+1) + D_s = 0$$

$$\left(\frac{rq'}{q} \right)^2 + \frac{8\mu_0 rp'}{B_\phi^2} > 0 \quad \begin{array}{l} \text{Suydam's} \\ \text{criterion} \end{array}$$

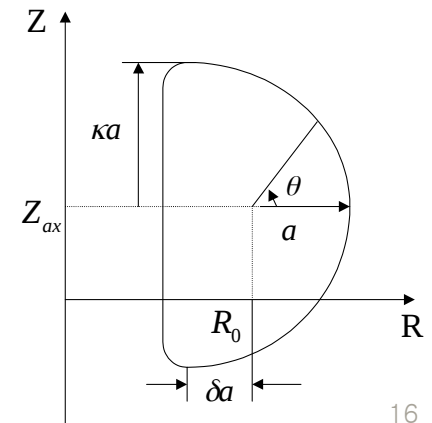
$$p_{1,2} = -\frac{1}{2} \pm \frac{1}{2} (1 - 4D_s)^{1/2}$$

For a circular cross section, large aspect ratio with $\beta_p \sim 1$

$$\left(\frac{rq'}{q} \right)^2 + 4r\beta'(1 - q^2) > 0 \quad \begin{array}{l} \text{Mercier} \\ \text{criterion} \end{array} \quad q_0 > 1$$

For a non-circular cross section

$$1 < q_0^2 \left\{ 1 - \frac{4}{1 + 3\kappa^2} \left[\frac{3\kappa^2 - 1}{4\kappa^2 + 1} \left(\kappa^2 - \frac{2\delta}{\varepsilon} \right) + \frac{(\kappa - 1)^2 \beta_{p0}}{\kappa(\kappa + 1)} \right] \right\}$$



Ideal MHD Instabilities

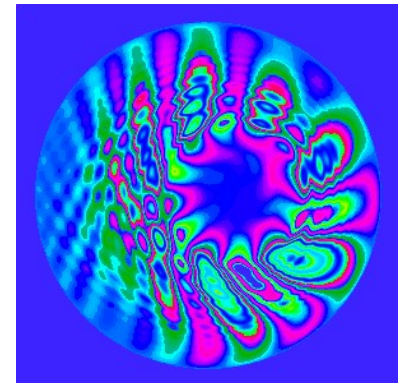
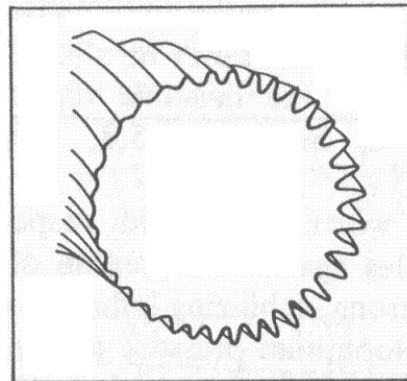
- **Ballooning Modes**

- driven by the pressure gradient at bad-curvature surface region
- localised high- n interchange mode at outbound edge of circular high- β tokamak or at the tips of an elongated plasma
- most dangerous and limiting MHD instability

- **Ballooning Modes**

- **Stabilising effects and stability conditions**

- keep $\beta < \beta_{\max} \approx \epsilon/q^2$
- strong magnetic shear
- noncircular plasma shape
- conducting wall



Ideal MHD Instabilities

- Analytic model

$$\frac{\partial}{\partial \theta} \left[(1 + \Lambda^2) \frac{\partial X}{\partial \theta} \right] + \alpha (\Lambda \sin \theta + \cos \theta) X = 0$$

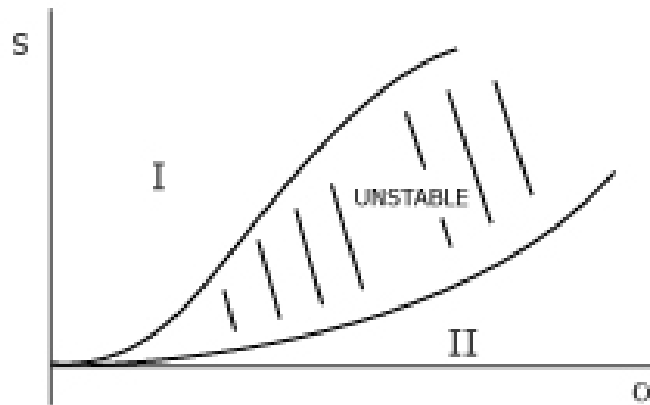
desired form of the ballooning mode equation for the model equilibrium (s, α)

$$\Lambda(\theta) = s(\theta - \theta_0) - \alpha(\sin \theta - \sin \theta_0)$$

$$s = \frac{rq'}{q} \quad \text{average shear}$$

$$\alpha = - \frac{2\mu_0 r^2 p'}{R_0 B_\theta^2} = - \frac{r^2 B_0^2}{R_0^2 B_\theta^2} \cdot R_0 \cdot \frac{p'}{B_0^2 / 2\mu_0} = - q^2 R_0 \beta'$$

measure of the pressure gradient



(s, α) diagram

Ideal MHD Instabilities

- **Numerical Results: the Sykes Limit, the Troyon Limit**

Once an equilibrium is established, the following stability tests are made.

- (1) Mercier stability
- (2) High- n ballooning modes
- (3) Low- n internal modes
- (4) External ballooning-kink modes

- Helpful in the design of new experiments and in the interpretation and analysis of existing experimental data
- Playing a role in the determination of optimised configurations
- Quantitative predictions for the maximum β_t or I_0 and that can be stably maintained in MHD equilibrium

$$\text{Troyon limit } \beta_t(\%) = \beta_N \frac{I_\phi(MA)}{a(m)B_\phi(R_0)(T)}$$

Ideal MHD Instabilities

- Limit on β due to ideal MHD instabilities

$$\beta = \frac{p}{B^2 / 2\mu_0} \approx \beta_p \left(\frac{B_\theta}{B_\phi} \right)^2 = \beta_p \left(\frac{\kappa a / R_0}{q(a)} \right)^2$$
$$= \kappa \left(\frac{a}{R_0} \beta_p \right) \left(\frac{\kappa a}{R_0} \right) \left(\frac{q(0)}{q(a)} \right)^2 \left(\frac{1}{q(0)} \right)^2$$

(1) (2) (3) (4) (5)

(1): vertical instability limit

(2) ≤ 1 : ballooning mode limit

(3) $\leq 1/3$: space limit (geometry, shielding, maintenance, heating, etc)

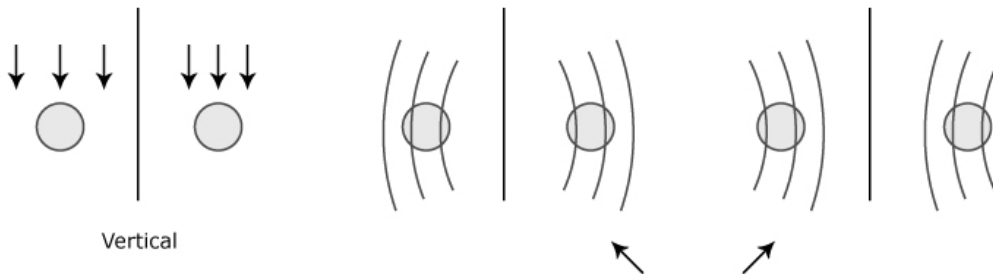
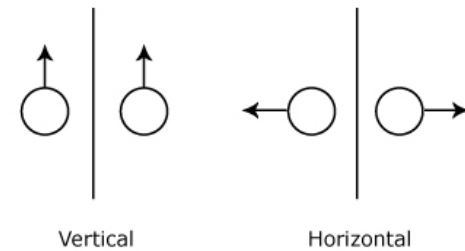
(4) ≤ 0.2 : surface kinks

(5) ≤ 1 : internal modes

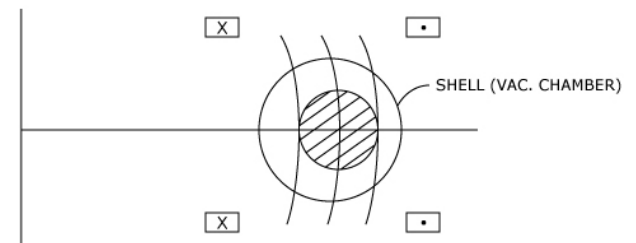
Ideal MHD Instabilities

- **Vertical Instability**

- $n = 0$ axisymmetric modes:
macroscopic motion of the plasma towards the wall



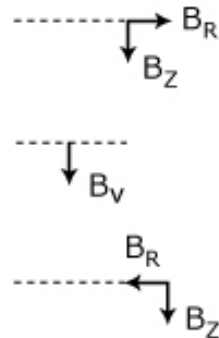
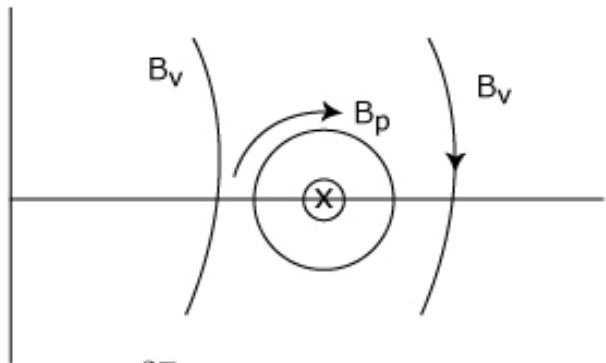
Which is good for stability?



Ideal MHD Instabilities

• Vertical Instability

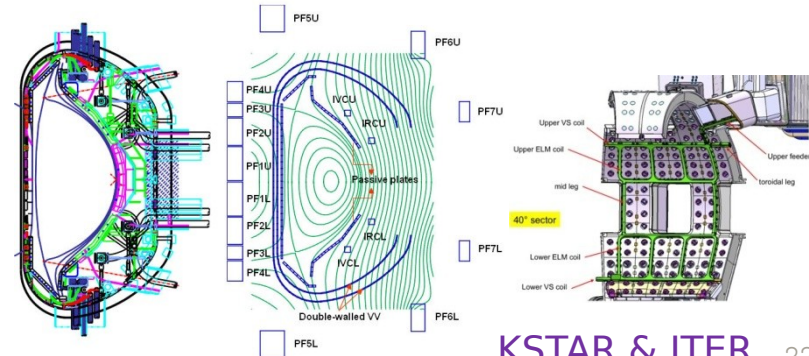
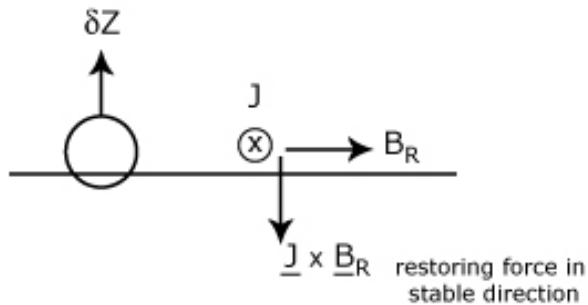
- For a circular cross sections a moderate shaping of the vertical field should provide stability.
- For noncircular tokamaks, vertical instabilities produce important limitations on the maximum achievable elongations.
- Even moderate elongations require a conducting wall or a feedback system for vertical stability.



field index

$$n(R_0, Z_0) = - \left(\frac{R}{B_Z} \frac{\partial B_Z}{\partial R} \right)_{R_0, Z_0}$$

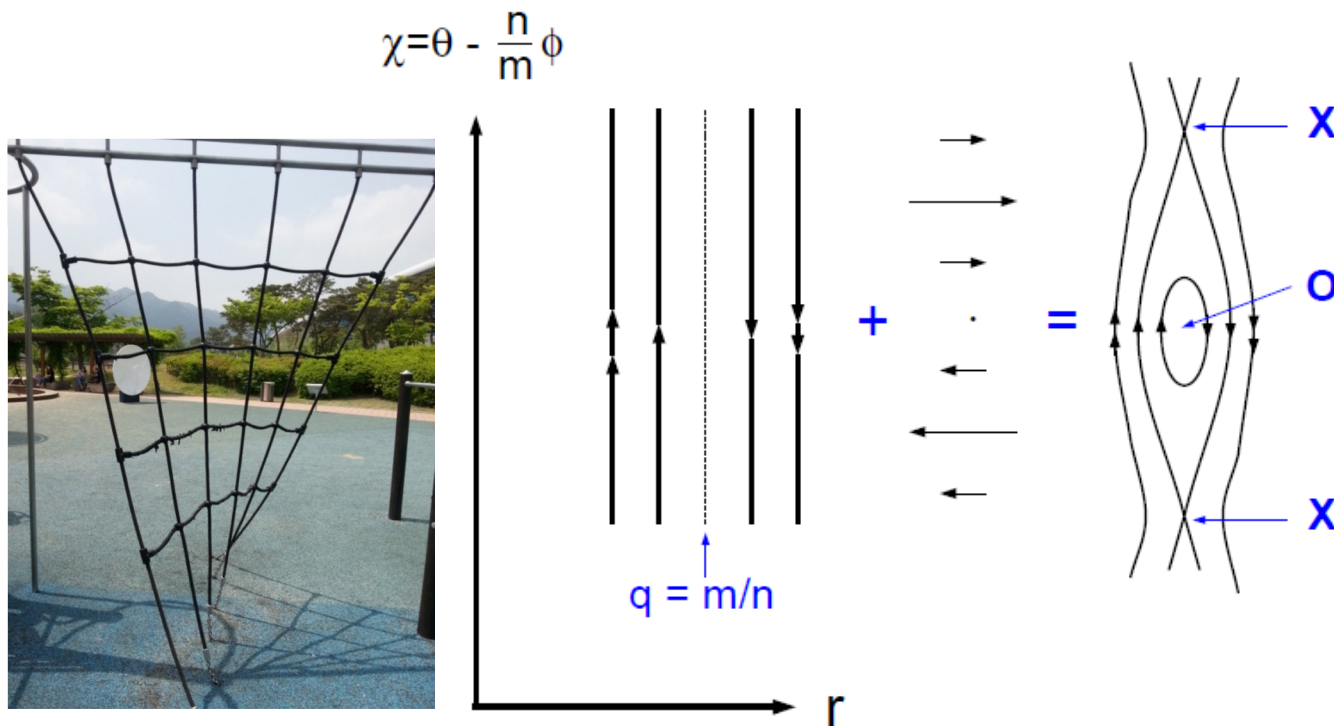
$$0 < n < 3/2$$



KSTAR & ITER

Resistive MHD Instabilities

- growing more slowly compared with the ideal instabilities (10^{-4} - 10^{-2} s)
- resulting from the diffusion or tearing of the magnetic field lines relative to the plasma fluid
- destroying the nested topology of the magnetic flux surfaces



Resistive MHD Instabilities

- **Tearing Modes**

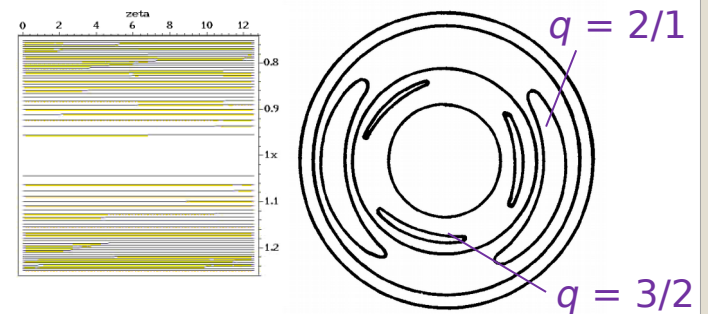
- resistive internal kink modes ($m \geq 2$)
- driven by perturbed \mathbf{B} induced by current layer (∇J) in plasmas
- magnetic island formation
- mode rational surface $r = r_s$ where $q(r_s) = m/n$ falls in plasmas
- saturation at some fraction of plasma width (\sim a few tenths of plasma radius a)
- growth rate $\gamma \propto \pi^{1/3}$
- more tolerable and lower than ideal modes

- **Tearing Modes**

- **Stabilising effects and stability conditions**

- unstable region reduced as sharpness of the current profile v increases
 - m increases
 - closeness of the wall to the plasma
 - $q(a)/q(0)$ (shear) increases
- stability condition:

$$q_0 > 3$$



Microinstabilities

- often associated with non-Maxwellian velocity distributions: deviation from thermodynamic equilibrium (nonuniformity, anisotropy of distributions) → free energy source which can drive instabilities
- kinetic approach required: limited MHD approach
- driving anomalous transports
- **Two-stream or beam-plasma instability**
 - Particle bunching → \mathbf{E} perturbation → bunching ↑ → unstable
- **Drift (or Universal) instability**
 - driven by ∇p (or ∇n) in magnetic field
 - excited by drift waves with a phase velocity of v_{De} with a very short wavelength
 - most unstable, dominant for anomalous transport
 - stabilisation: good curvature (min- \mathbf{B}), shear, finite β
- **Trapped particle modes**
 - anisotropy due to passing particles having large $v_{||}$ among trapped ones
 - Preferably when the perturbation frequency $<$ bounce frequency
 - increasing cross-field diffusion
 - drift instability enhanced by trapped particle effects
 - Trapped Electron Mode (TEM), Trapped Ion Mode (TIM)

Non-linear Plasma Activity

- Sawtooth

VOLUME 33, NUMBER 20

PHYSICAL REVIEW LETTERS

11 NOVEMBER 1974

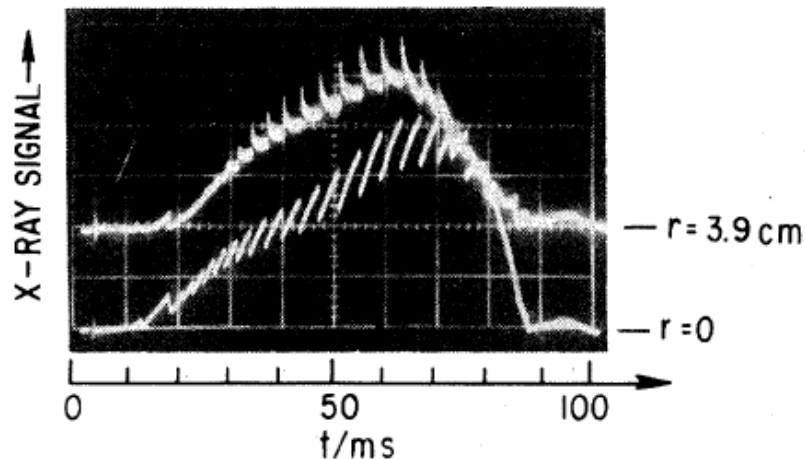
Studies of Internal Disruptions and $m = 1$ Oscillations in Tokamak Discharges with Soft-X-Ray Techniques*

S. von Goeler, W. Stodiek, and N. Sauthoff

Plasma Physics Laboratory, Princeton University, Princeton, New Jersey 08540

(Received 11 July 1974)

Fluctuations in x-ray intensity from the ST tokamak show a characteristic sawtooth behavior. This behavior is identified as an internal disruption. The internal disruptions are preceded by growing sinusoidal $m = 1, n = 1$ oscillations. The properties of these oscillations are compared with predictions for the $m = 1$ internal kink mode.



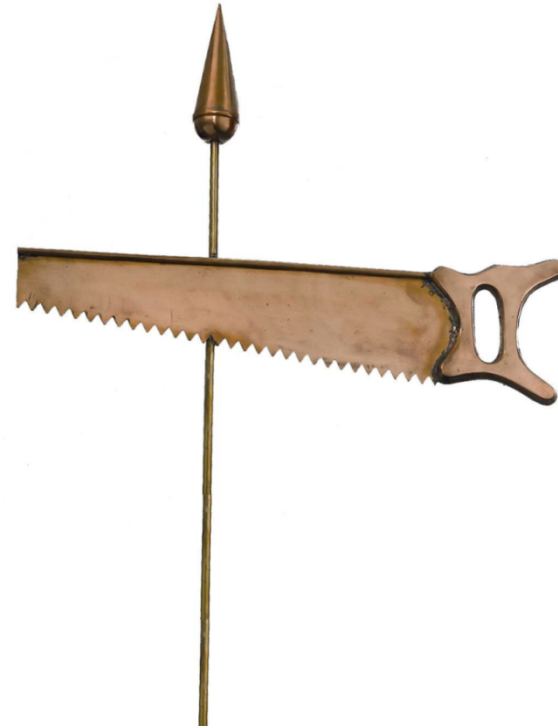
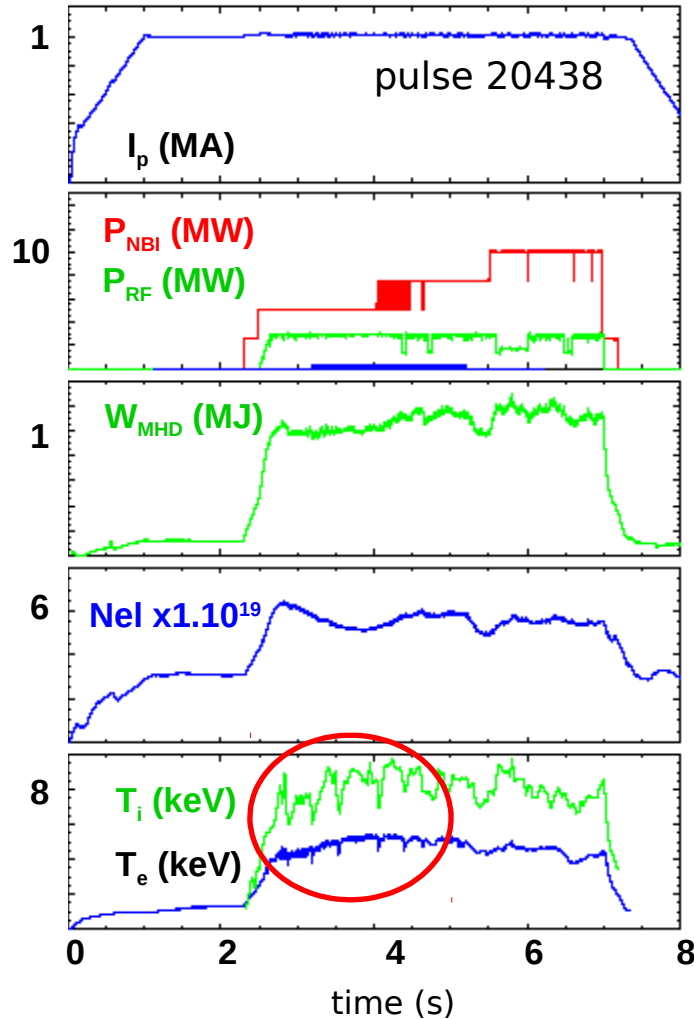
of the plasma electrons and consists predominantly of the recombination-radiation continuum of the partly ionized oxygen and iron impurities.¹ The radiation intensity is therefore a function of the electron density and temperature and of the impurity concentration. The x-ray fluctuations are caused by a fluctuation in either of these quantities, but predominantly by temperature fluctuations.

The oscillograms of the x-ray emissions, shown in Fig. 1, are typical for high-density discharges in the ST tokamak. The traces exhibit a “sawtoothlike” oscillation. The sawtooth is “inverted,” showing a fast rise and a slow exponential drop,

Non-linear Plasma Activity



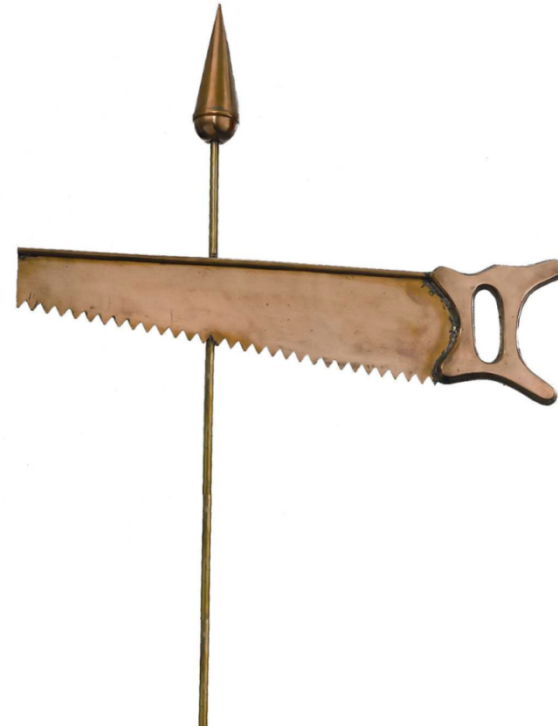
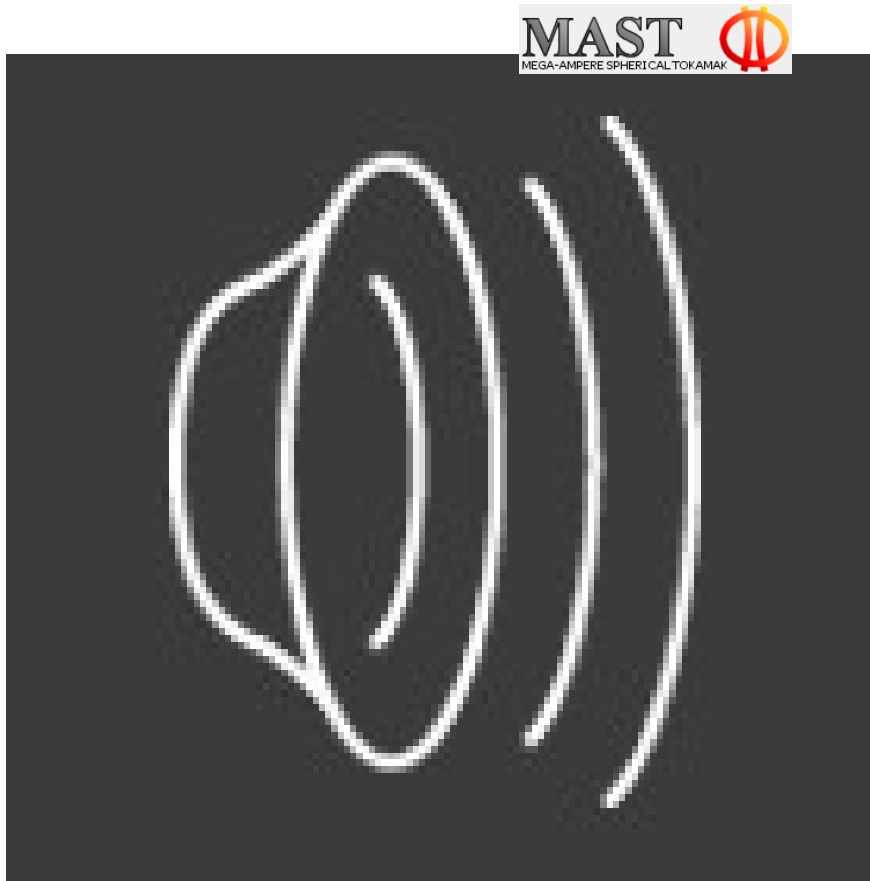
- Sawtooth



- non-linear low- n internal mode
- internal (minor) disruption
- increased energy transport in the plasma centre

Non-linear Plasma Activity

- Sawtooth



IT Chapman et al, PRL, 2010

Non-linear Plasma Activity

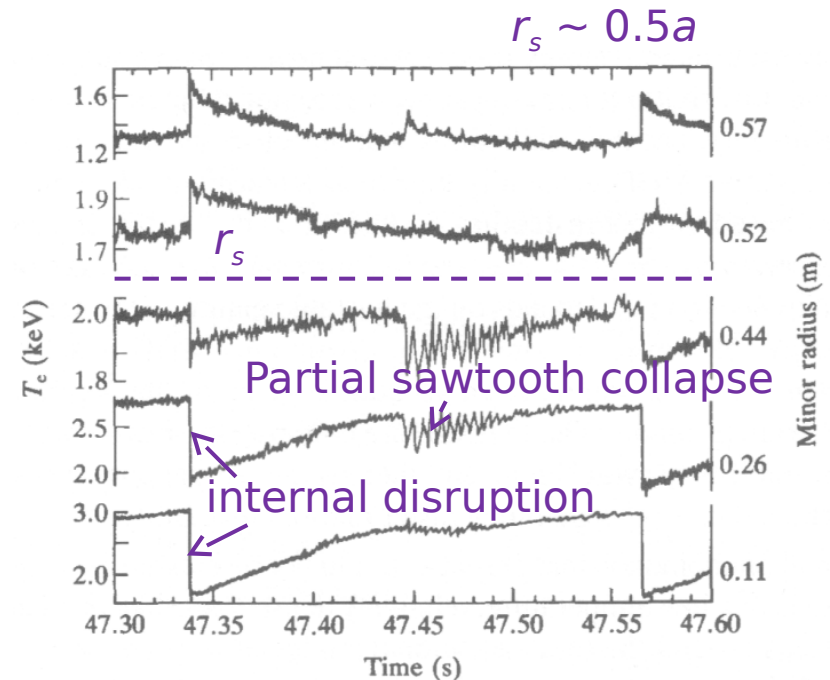
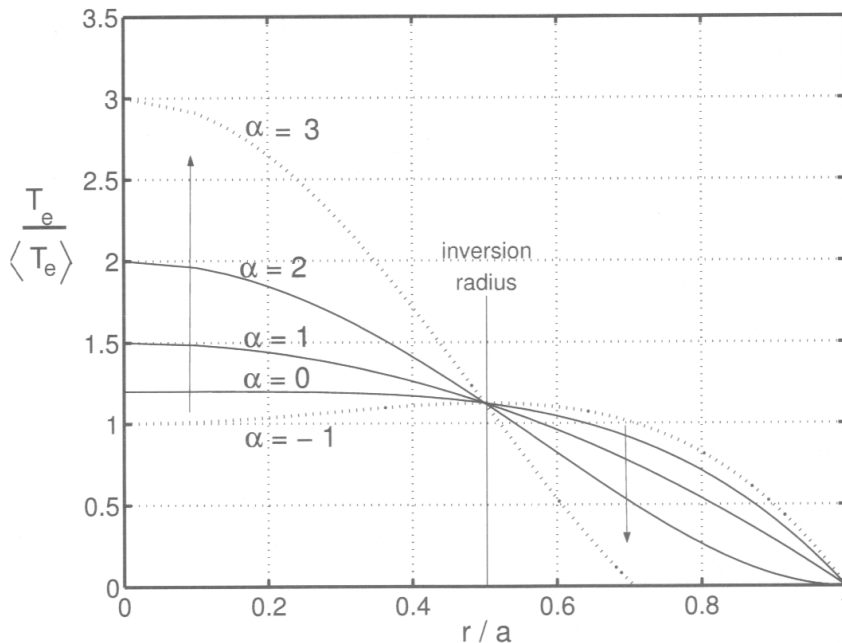
- **Sawtooth**

- It occurs so commonly that its presence is accepted as a signal that the tokamak is operating normally.
- Important type of plasma non-linear activity
 - Decreasing the thermal insulation
 - Key to understanding the disruptive instability
- Consisting of periodically repeated phases of
 - slow temperature rise at the centre of the plasma column
 - fast drop ($m = 1, n = 1$ oscillatory MHD modes oscillation precursors observed before the drop)

Non-linear Plasma Activity

- **Sawtooth**

- Inversion radius (r_s): when central temperature drops and flattens, the temperature decreases inside the radius and increases directly beyond it.



$$T_e = T_{e0} \left[1 - \alpha y - (1 - \alpha) y^2 \right], \quad T_{e0} = 6 \langle T_e \rangle / (5 - \alpha)$$



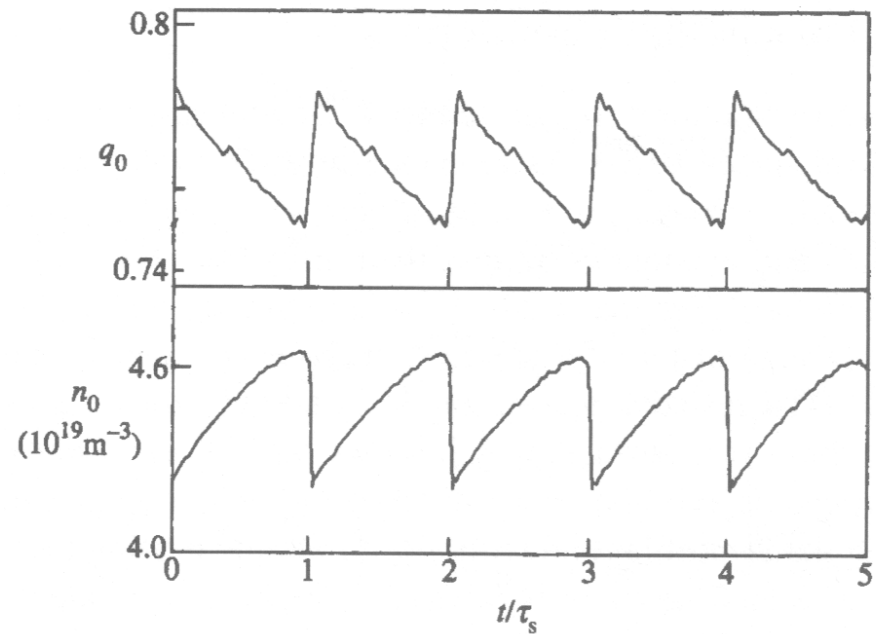
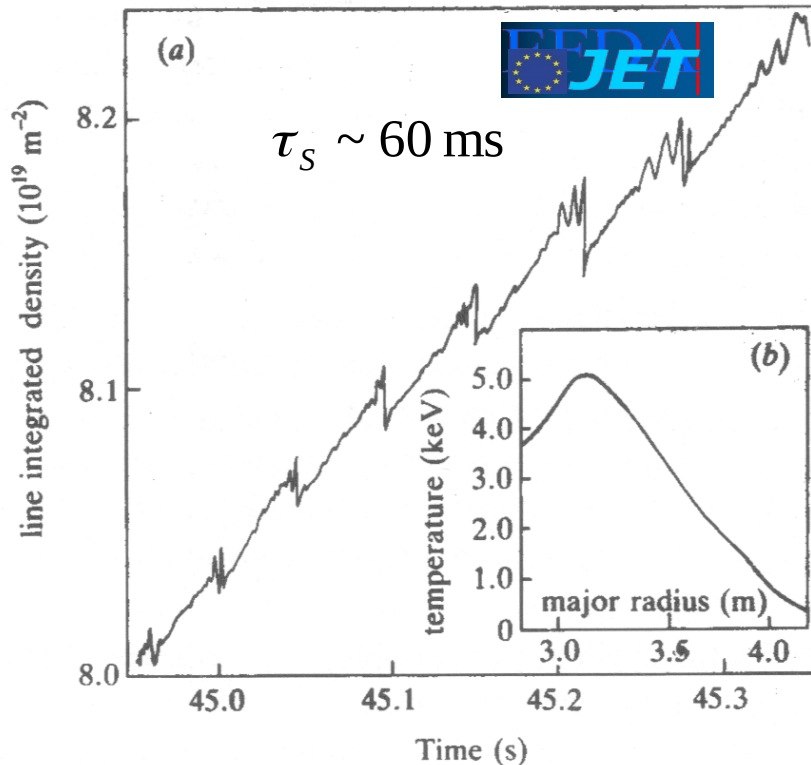
Non-linear Plasma Activity

- Sawtooth**

- $\Delta T_e \sim 40\%$, $\Delta q_0 \sim 4\%$, $\Delta n_0 \sim 9\%$



TEXTOR
(H. Soltwisch et al, APS (1987))



- Simple semi-empirical scaling for the period of sawtooth oscillations

$$\tau_s \approx 10^{-2} R^2 T_e^{3/2} / Z_{\text{eff}}$$

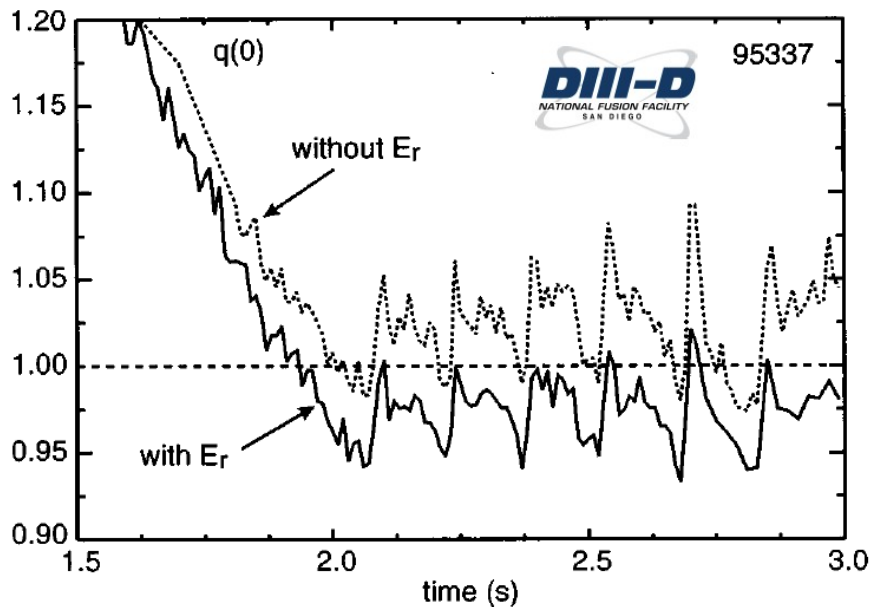
Non-linear Plasma Activity

- **Sawtooth**

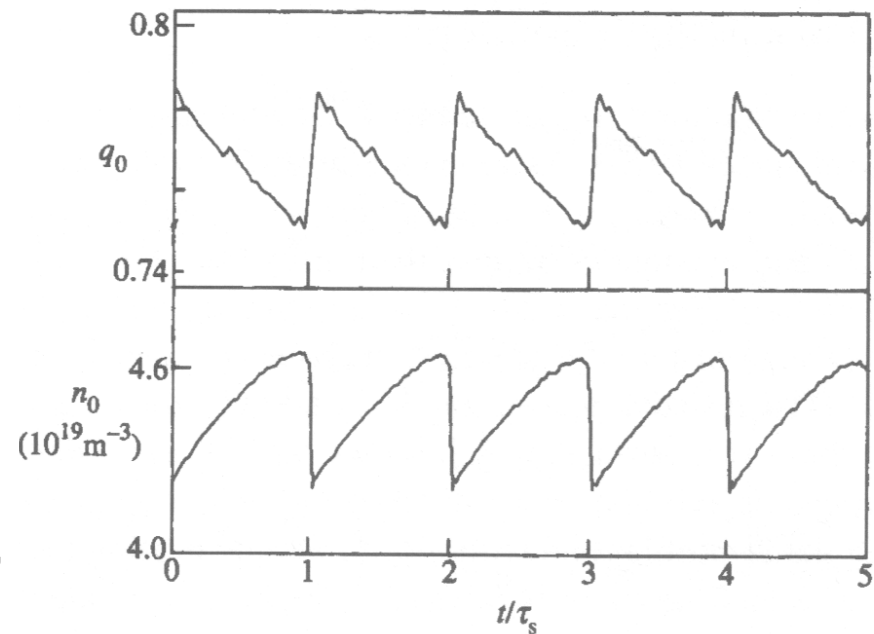
- $\Delta T_e \sim 40\%$, $\Delta q_0 \sim 4\%$, $\Delta n_0 \sim 9\%$



TEXTOR
(H. Soltwisch et al, APS (1987))



B. W. Rice et al., *Rev. Sci. Instrum.* **70** 815 (1999)



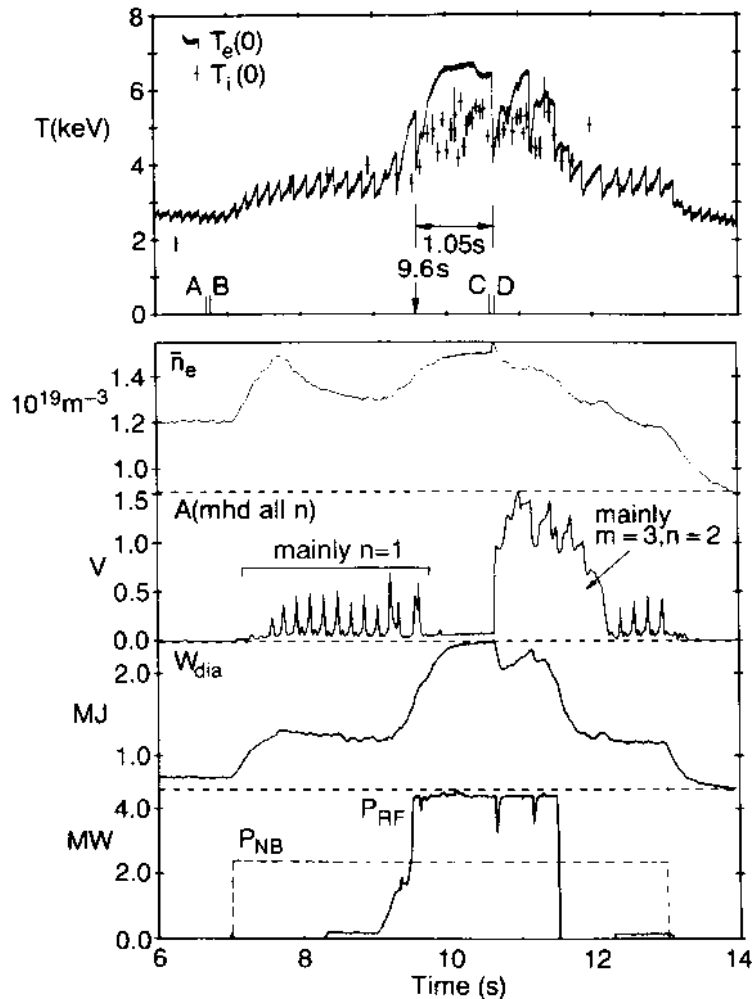
- Simple semi-empirical scaling for the period of sawtooth oscillations

$$\tau_s \approx 10^{-2} R^2 T_e^{3/2} / Z_{eff}$$

Non-linear Plasma Activity

- **Monster Sawtooth**

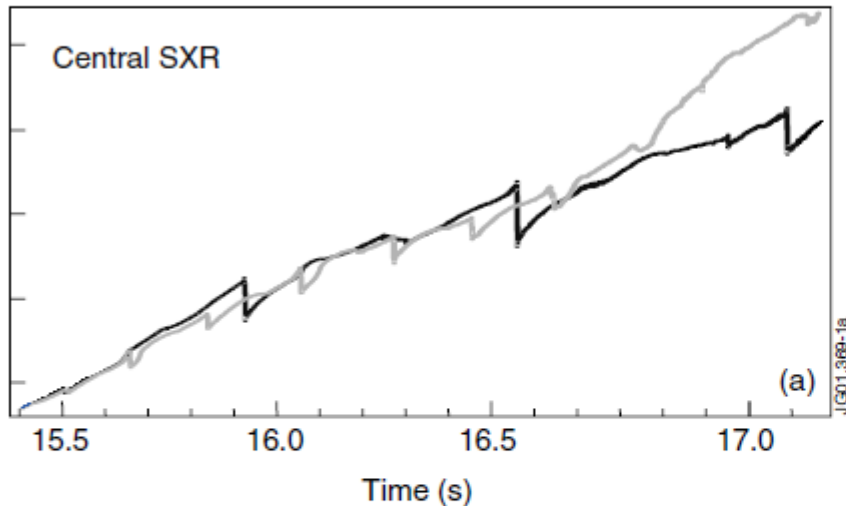
- No low (m,n) number coherent MHD activity observed during the temperature saturation phase
- ICRH and/or NBI above 5 MW
- Possibly due to stabilisation of the $m = 1$ instability by fast ions



D. J. Campbell et al, PRL 60 2148 (1988)

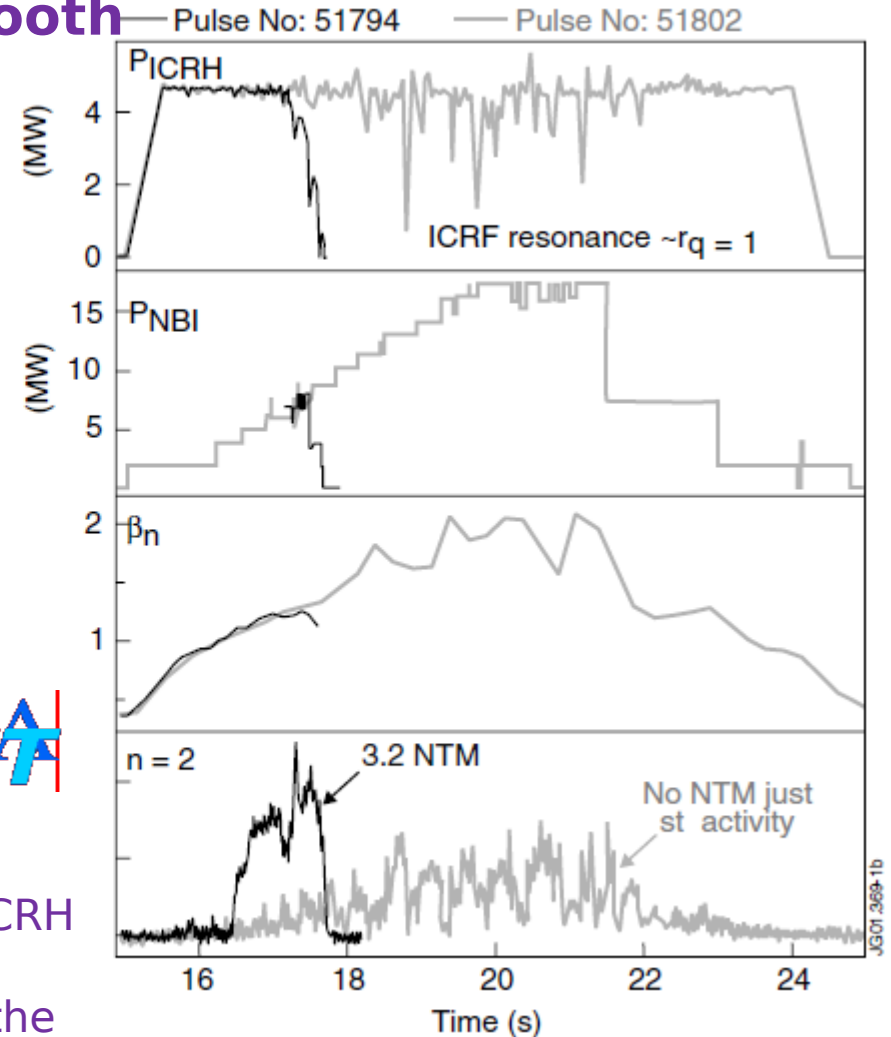
Non-linear Plasma Activity

- NTM triggered by Sawtooth



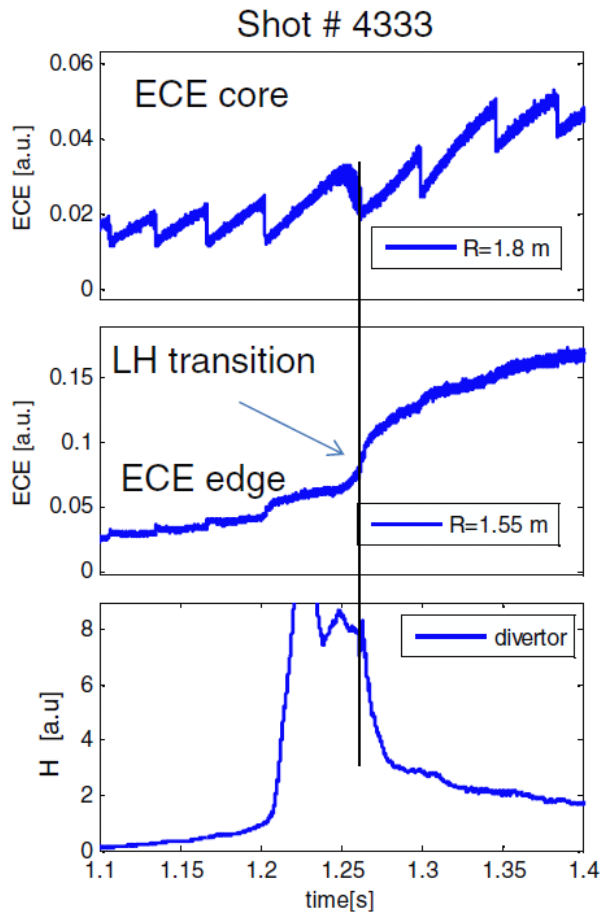
EFDA
JET

- Increased sawtooth period due to stabilisation by fast ions produced by ICRH leads to the triggering of $n = 2$ NTM activity which causes a termination of the discharge.



Non-linear Plasma Activity

- Sawtooth
 - Sawtooth triggered L-H transition



Non-linear Plasma Activity

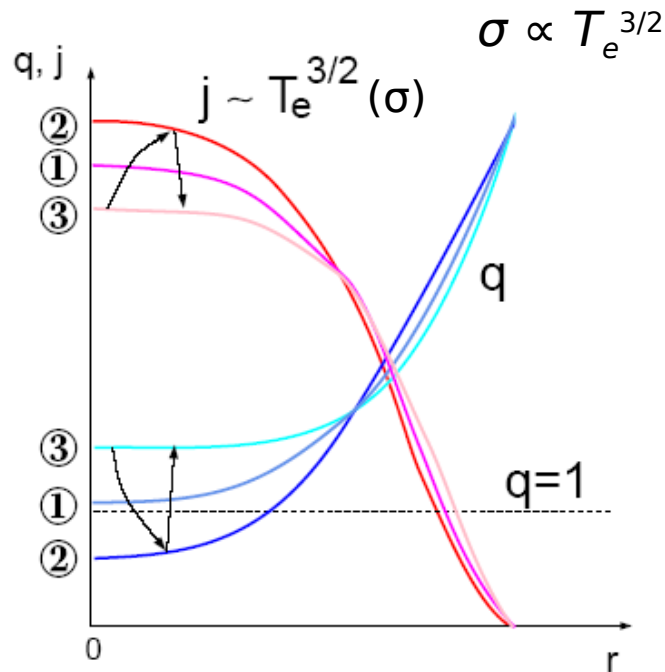
- **Sawtooth**

- Why the sawtooth oscillation should occur at all has not yet been explained.
- Two instabilities are required to drive the process
 - abrupt collapse
 - ramp phase

Non-linear Plasma Activity

- **Sawtooth**

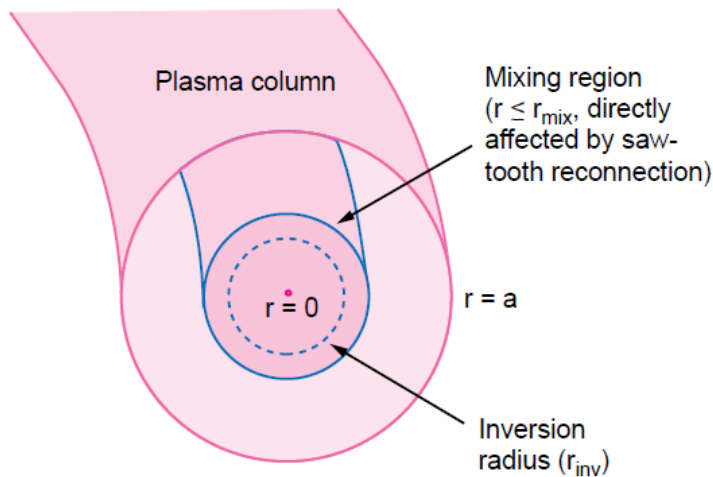
- Kadomtsev model



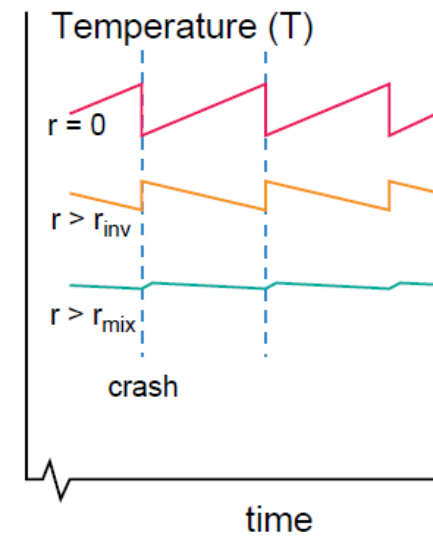
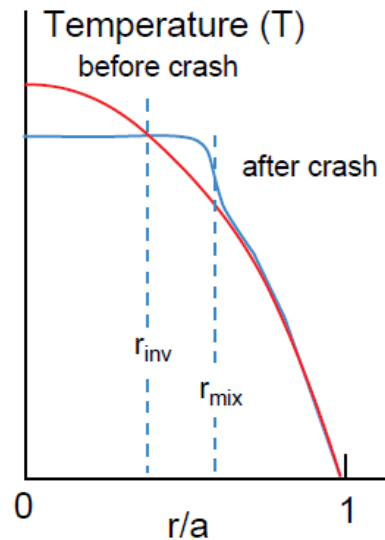
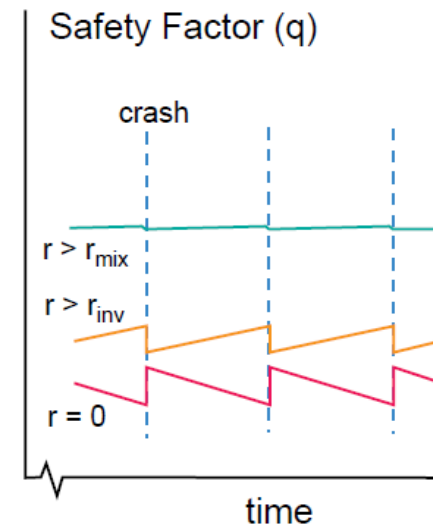
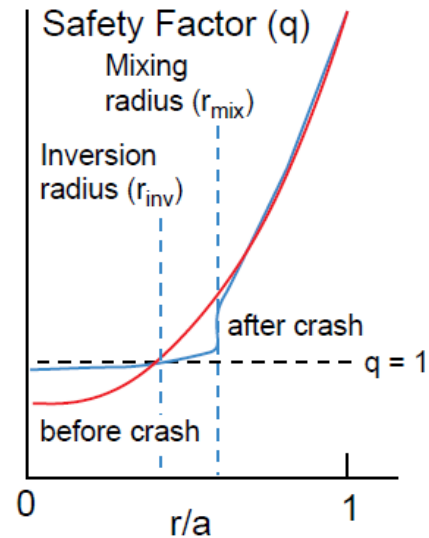
1. $T(0)$ and $j(0)$ rise due to ohmic heating (slower phase, resistive time scale)
2. $q(0)$ falls below 1, $q(r_s) = 1$
→ kink instability ($m/n=1/1$) grows
3. Fast reconnection event:
 T, n flattened inside $q = 1$ surface
 $q(0)$ rises slightly above 1
kink stable

Non-linear Plasma Activity

- Sawtooth**



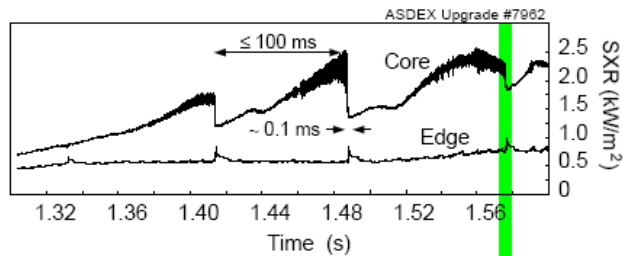
ITER Physics Basis NF (1999)



Non-linear Plasma Activity

- Sawtooth**

- Kadomtsev model

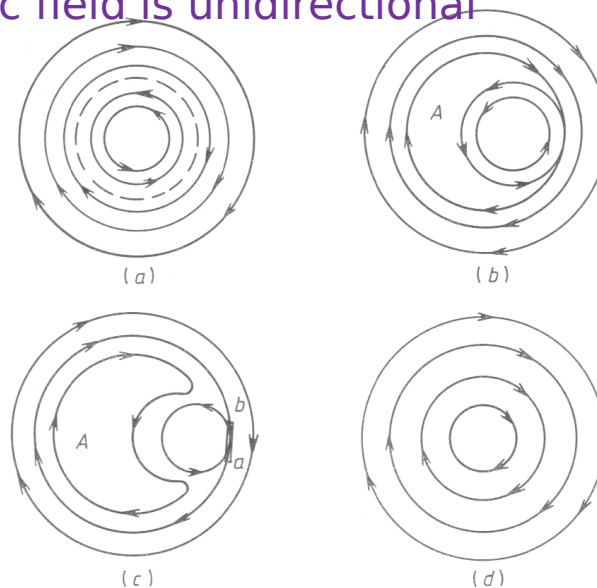
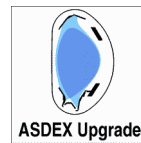
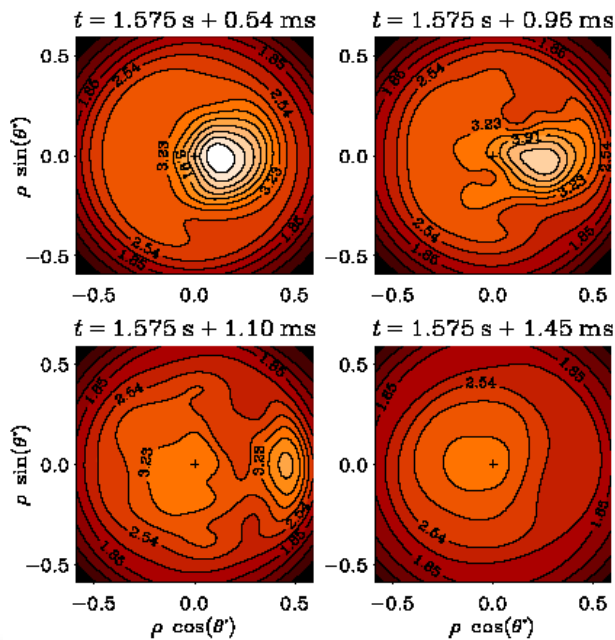


(a) auxiliary transverse field $B_* = B_\theta - (r/R)B_T$ (different direction of magnetic lines relative to the surface with $B_* = 0$ ($q = 1$))

(b) contact of surfaces with oppositely directed fields B_*

(c) reconnection of the current layer ab due to finite plasma conductivity. A moon-like island A formed due to the reconnection

(d) final result of reconnections: auxiliary magnetic field is unidirectional



Non-linear Plasma Activity

- **Sawtooth**

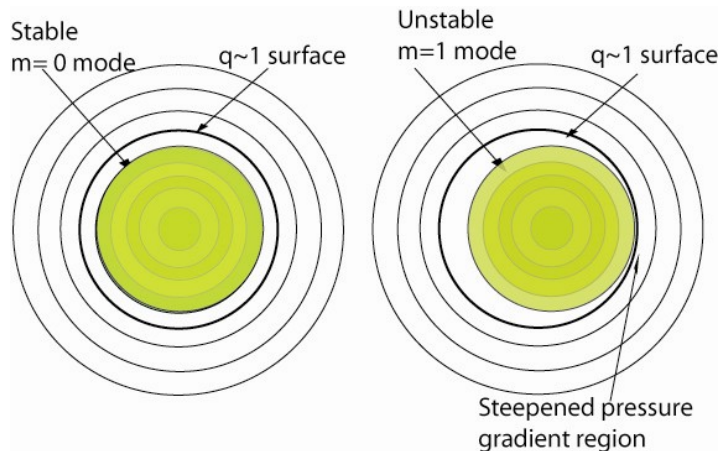
- Kadomtsev model

(a) the plasma current density in the core region increases ($q(0)$ drops below unity), and the $m/n=1/1$ internal kink mode becomes unstable due to a pressure driven instability.

(b) Island formation starts due to an influx of the cooler part of the plasma outside the inversion radius through the magnetic reconnection as soon as the pressure driven instability reconnects the magnetic field through the reconnection zone along the magnetic pitch of the $q\sim 1$ surface.

(c) As the island (the region with $q\sim 1$) grows, the hot spot (the region with $q<1$) gets smaller and it is eventually eliminated.

(d) The island fully occupies the core on a reconnection time scale defined as $T_c \sim 0.5(\tau_A^* \tau_\eta)$, where τ_A^* is the modified Alfvén transit time and τ_η is the resistive diffusion time.



Non-linear Plasma Activity

- **Sawtooth**

- Reconnection of the magnetic field lines: Sweet-Parker model

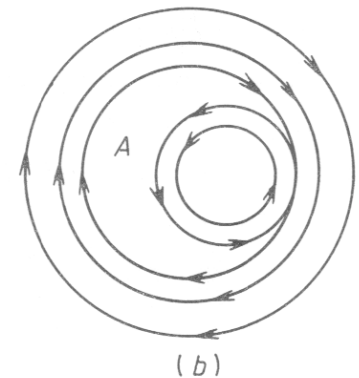
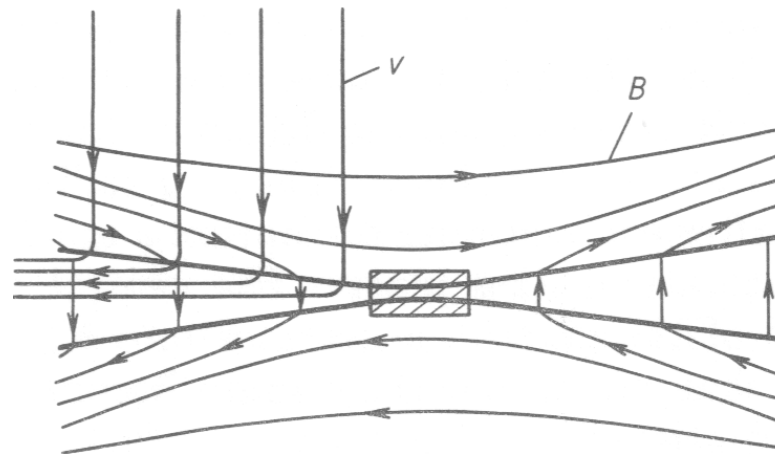
1. Magnetic fields are pushed together by flows into a narrow region. In the flow regions the resistivity is low and hence the magnetic field is frozen in the flow. The two regions are separated by a current sheet (the reversal of the magnetic field requires a current to flow in the thin layer separating them). Within this layer resistive diffusion plays a key role.
2. As the two regions come together the plasma is squeezed out along the field lines allowing the fields to get closer and closer to the neutral sheet.
3. At some stage the field lines break and reconnect in a new configuration at a magnetic null-point, X . The large stresses in the acutely bent field lines in the vicinity of the null-point result in a double-action magnetic 'catapult' that ejects plasma in both directions, with velocity of $O(v_A)$. This in turn allows plasma to flow into the reconnection zone from the sides.

Non-linear Plasma Activity

- **Sawtooth**

- Reconnection of the magnetic field lines: Sweet-Parker model

1. The field diffuses into plasma and magnetic lines reconnect.
2. A kind of 'catapult' of strained magnetic lines is formed.
3. It throws out the plasma from the layer into the moon-like region A of the magnetic island (b)

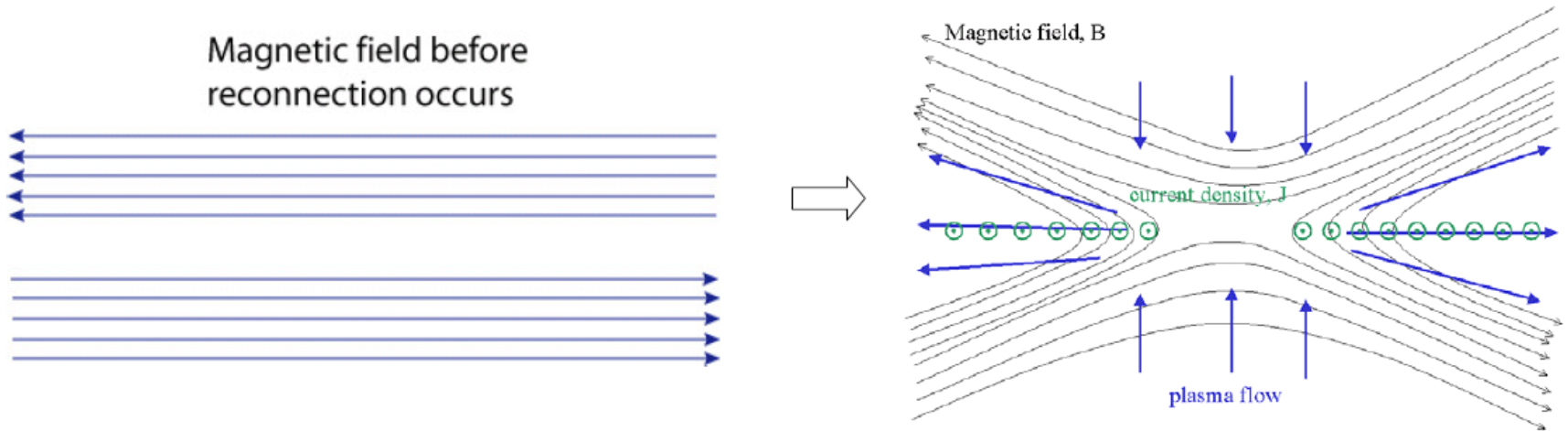


Non-linear Plasma Activity

- **Sawtooth**

- Reconnection of the magnetic field lines: Sweet-Parker model

1. The field diffuses into plasma and magnetic lines reconnect.
2. A kind of 'catapult' of strained magnetic lines is formed.
3. It throws out the plasma from the layer into the moon-like region A of the magnetic island (b)



Non-linear Plasma Activity

- **Sawtooth**

- Kadomtsev model

Shortcomings 1: collapse time for the disruption orders of magnitude longer than observed

$\tau_c = \omega^2 / \xi_{\perp}$ collapse time (ω : island width)

$$\xi_{\perp} = \frac{\eta}{\mu_0} = \frac{m_e}{\mu_0 e^2 n_e \tau_e} = 1.025 \times 10^8 \ln \Lambda / T_e^{3/2} \approx 4.4 \times 10^{-2} T_e^{3/2} \quad \text{magnetic diffusivity}$$

Ex) $\tau_c \sim 10$ ms at $\omega = 1$ cm, $T_e = 3$ keV

JET: $\tau_c = 50$ - 200 μ s but Kadomtsev model gives $\tau_c \geq 10$ ms

→ If the collapse is associated with a magnetic rearrangement an explanation of its rapidity was required.

Non-linear Plasma Activity

- **Sawtooth**

- Kadomtsev model

Shortcomings 2: could not explain the fast island formation

Shortcomings 3: no precise specification for the occurrence of a disruption

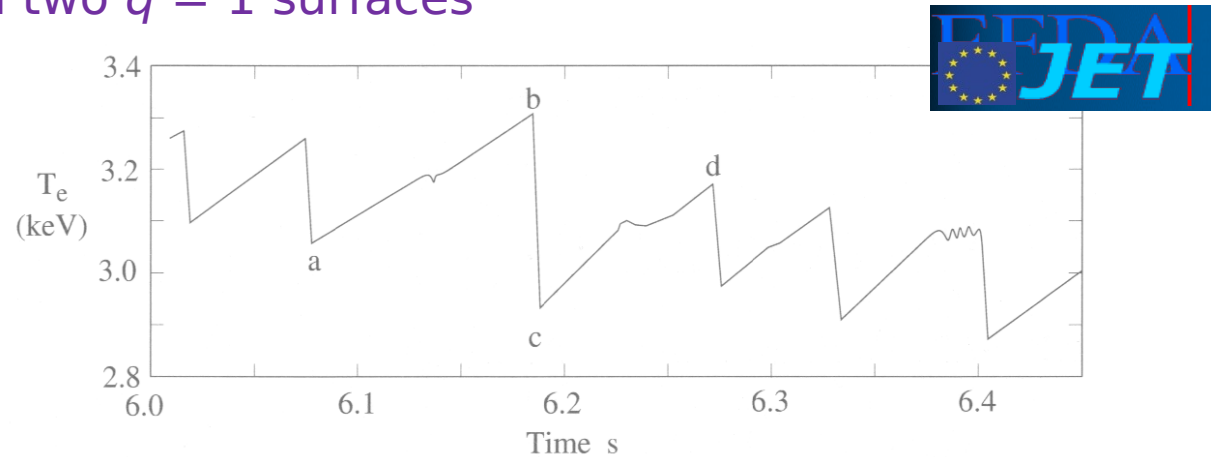
Shortcomings 4: sometimes expected precursors are absent or lacking in experiments as is the case with the large amplitude oscillations known as 'giant' or 'compound' sawteeth

Non-linear Plasma Activity

- **Sawtooth**

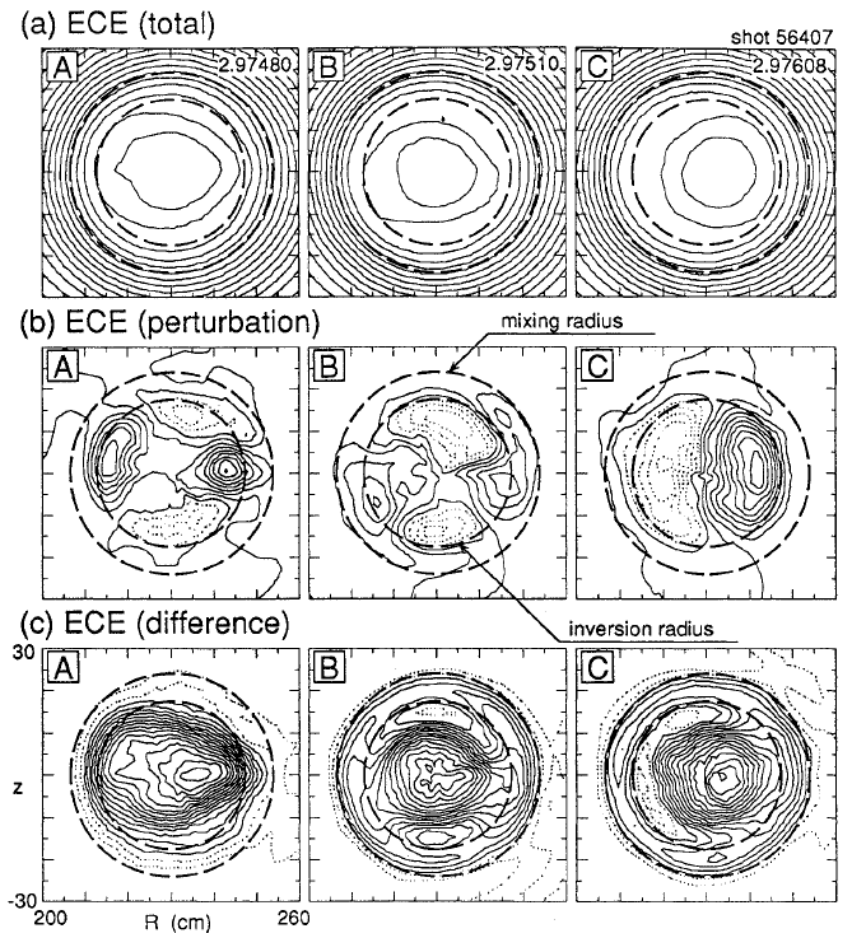
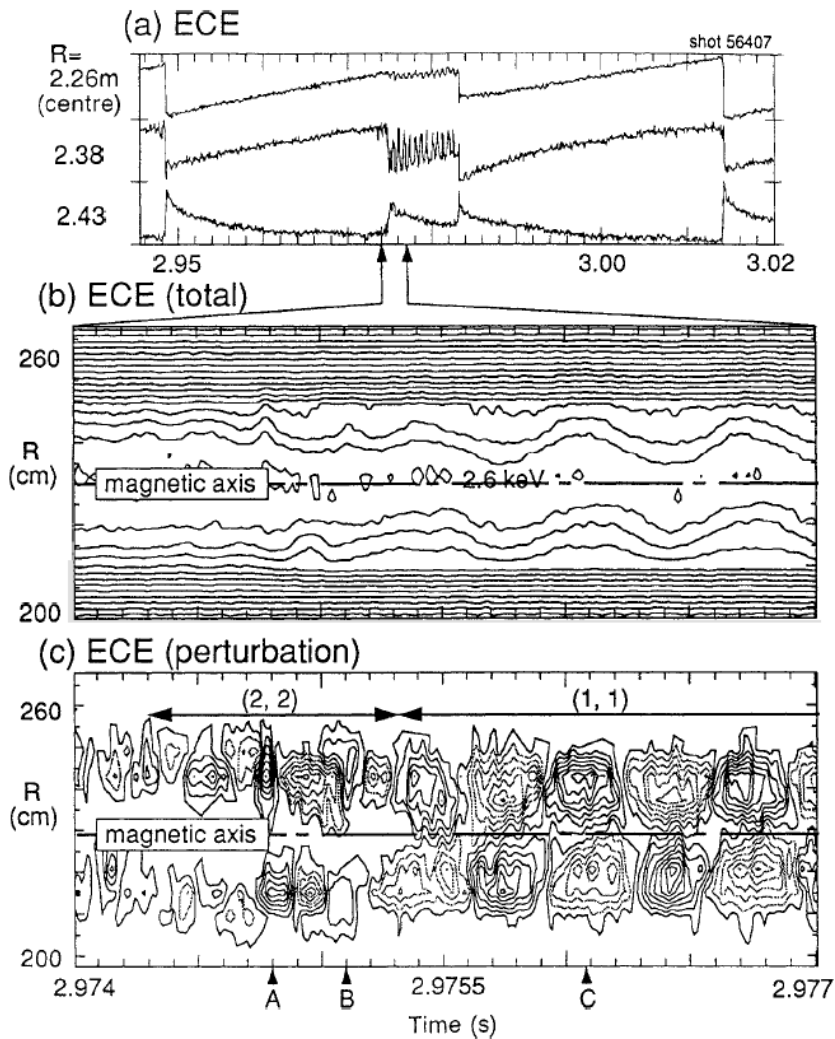
- Kadomtsev model

Shortcomings 5: existence of 'double' sawteeth with a longer and sometimes erratic period and a larger amplitude - requiring a hollow current profile with two $q = 1$ surfaces



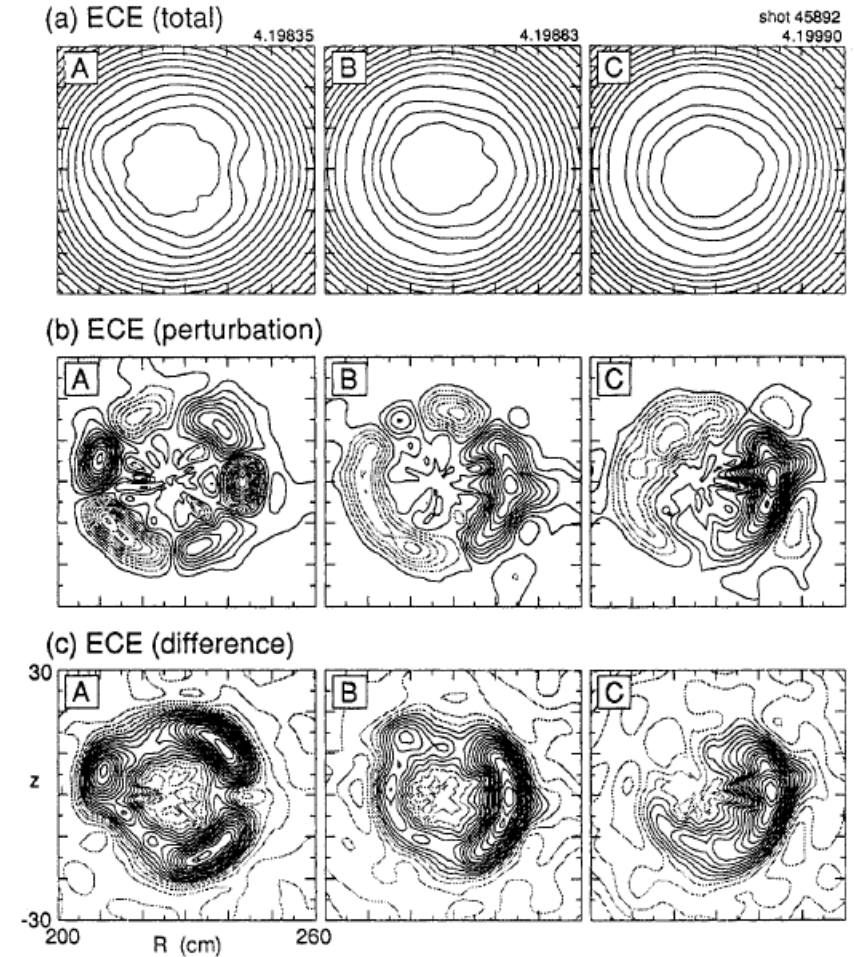
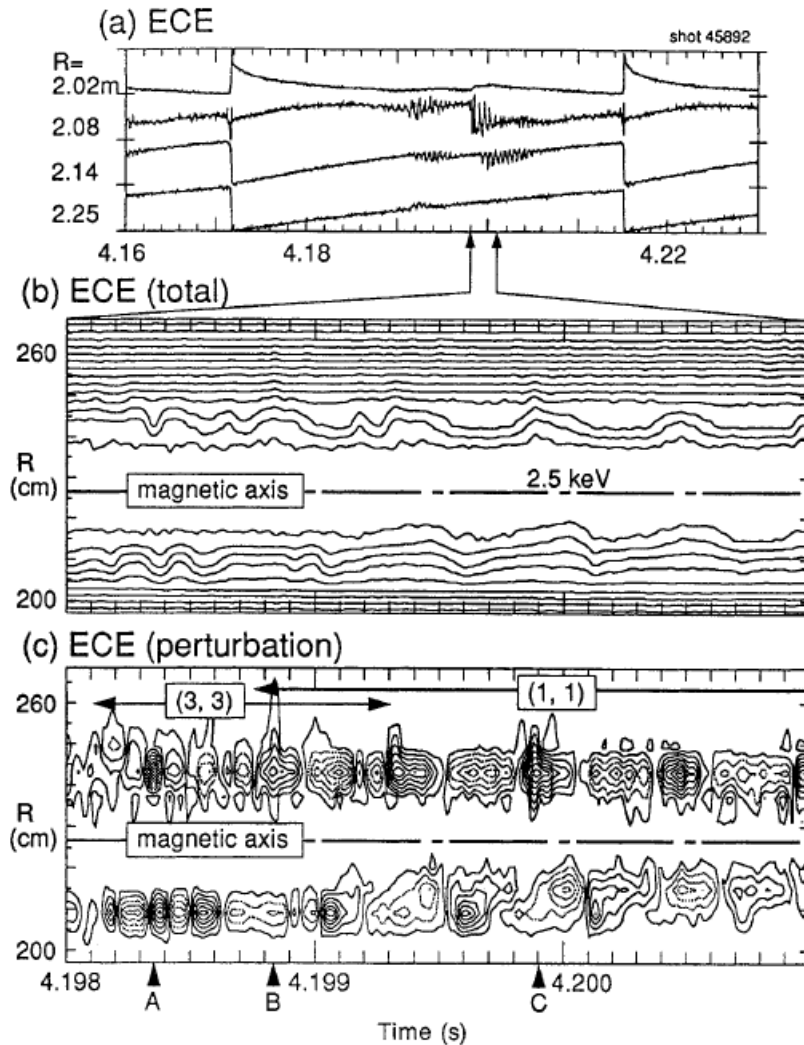
Non-linear Plasma Activity

- Partial crash by higher modes



Non-linear Plasma Activity

- Partial crash by higher modes

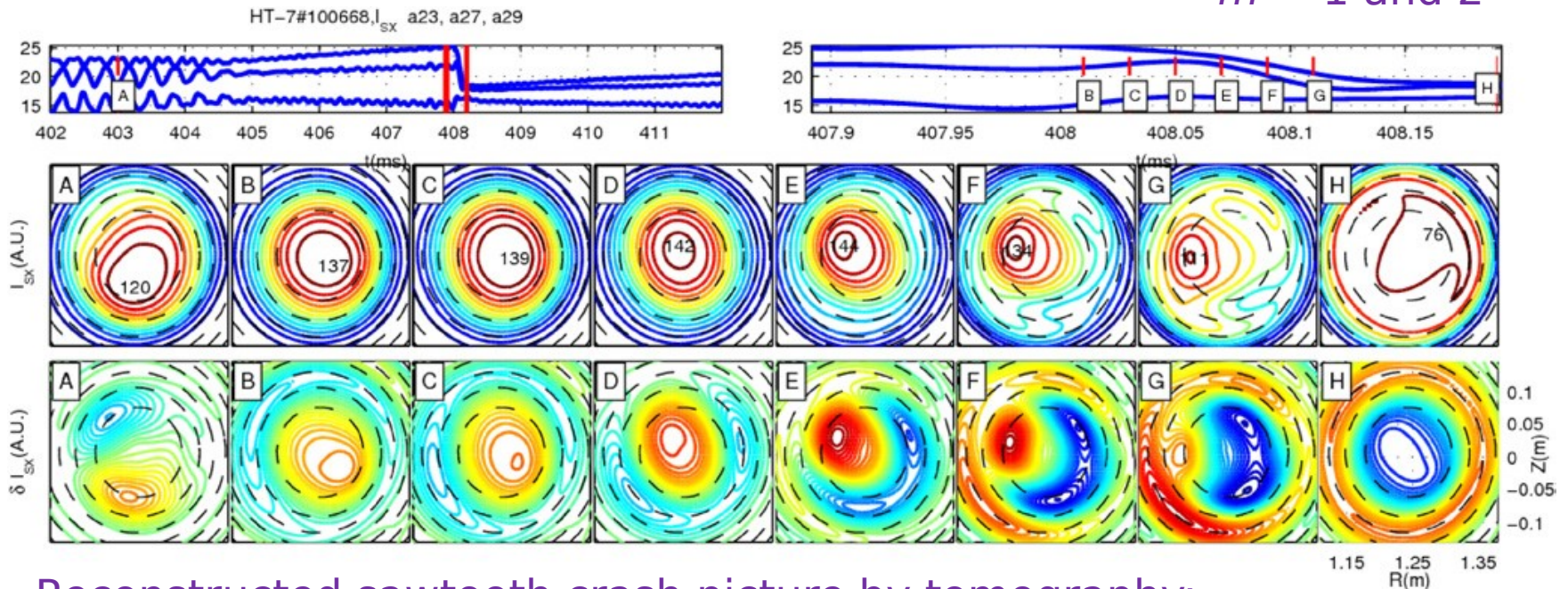


Y. Nagayama et al, NF 36 521 (1996)

Non-linear Plasma Activity

- Partial crash by higher modes

$m = 1$ and 2



- Reconstructed sawtooth crash picture by tomography:
line-integrated soft-x-ray signals at 3 chords,
the contour plot of the reconstructed local emission intensities profile from the total signals,
the contour plot of the reconstructed perturbation of the local emission intensities from the perturbation signals extracted by the SVD method

Youwen Sun et al, PPCF **51** 065001 (2009)

Non-linear Plasma Activity

- **Sawtooth**

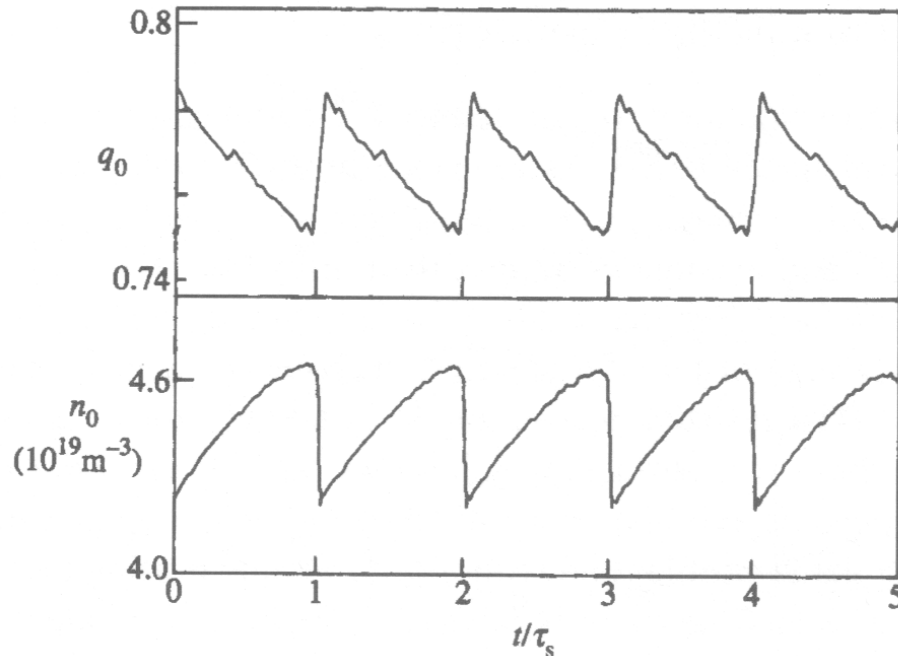
- Kadomtsev model

Shortcomings 6: q_0 remains below unity in many experiments



TEXTOR

(H. Soltwisch *et al*, Rev. Sci. Instrum. **59** 1599 (1988))



$q_0 < 1$ (~ 0.7) during all the sawtooth period
(F. M. Levinton *et al*, PRL **63** 2060 (1989))

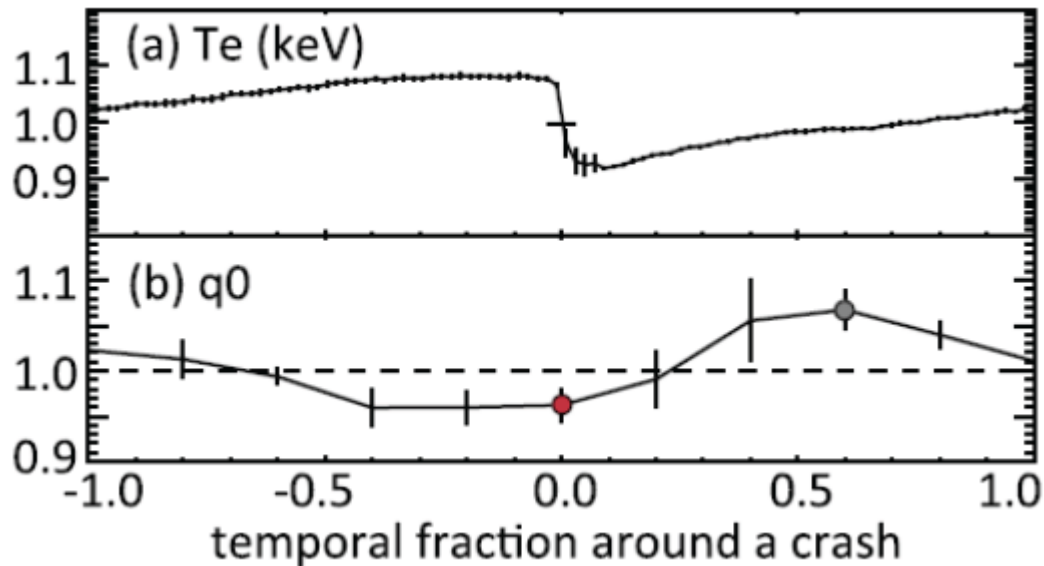
Any theory to explain $q_0 < 1$?

Non-linear Plasma Activity

- **Sawtooth**

- Kadomtsev model

Shortcomings 6: q_0 remains below unity in many experiments



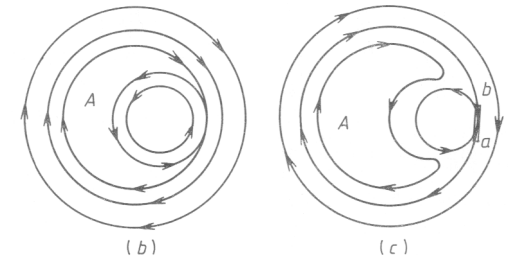
MSE measures $q_0 \sim 1.0 \pm 0.03$ with some uncertainties from E_r and κ .
(J. Ko, RSI 87 11E541 (2016))

Non-linear Plasma Activity

- **Sawtooth**

- Phase of the sharp temperature profile flattening (internal disruption)

1. What is the trigger of the internal disruption (type of instability)?
2. How does the disruption develop?
3. What is the time of disruption?



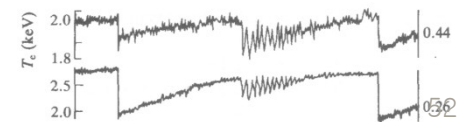
- Internal $m = 1/n = 1$ snake

- In some cases, instability occurs when β_p inside r_s exceeds a certain critical value.

- Every force tube 'catapulting' into A may drastically perturb plasma and create MHD-turbulence. If a turbulent zone is formed in A, then the B_* mean value may disappear due to mixing of magnetic lines.

Then there is no force that would 'press' the internal core to the magnetic surface with the inverse magnetic field.

→ partial (incomplete) reconnection



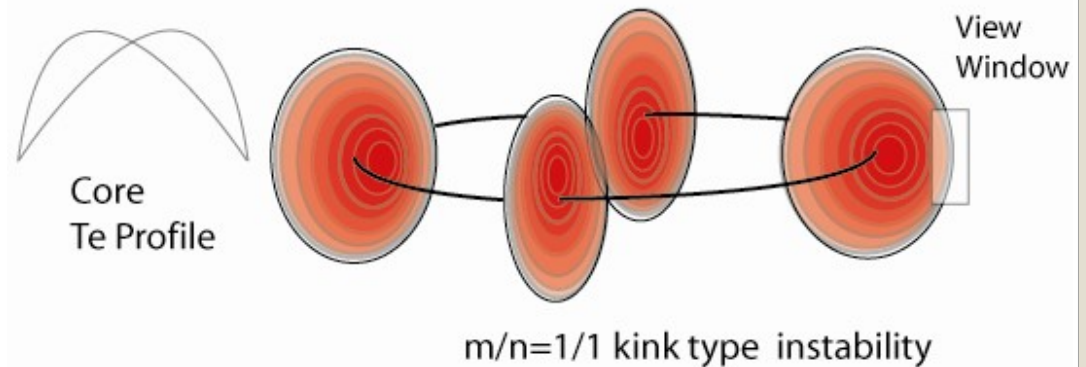
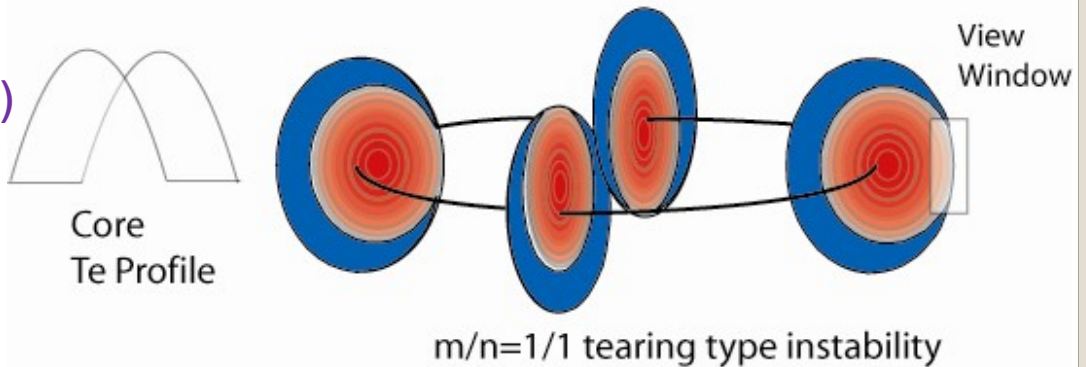
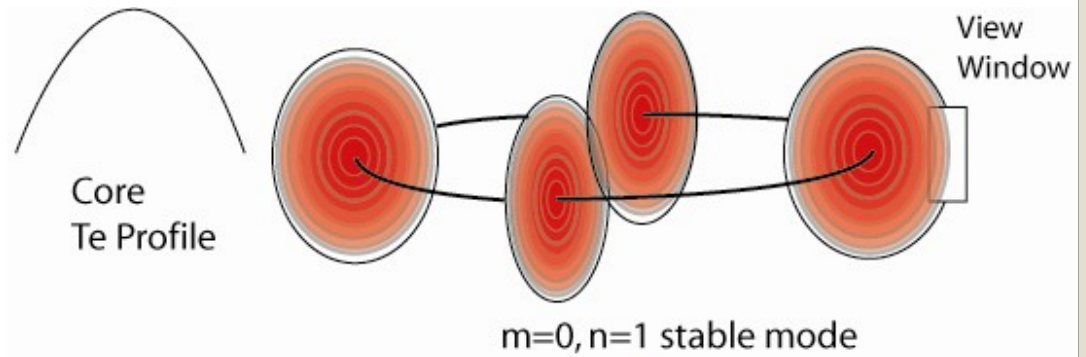
Non-linear Plasma Activity

- **Sawtooth**

- Stochasticity of the magnetic field lines may appear due to the toroidicity which violates the ideal helical symmetry.
 - change significantly the resistivity value inside the current layer
 - electron does not return back to the same point if after crossing the current layer, an anomalous skin-layer can develop.
 - significantly increasing the reconnection rate and makes it close to the observed one at the fastest internal disruptions.

Sawtooth

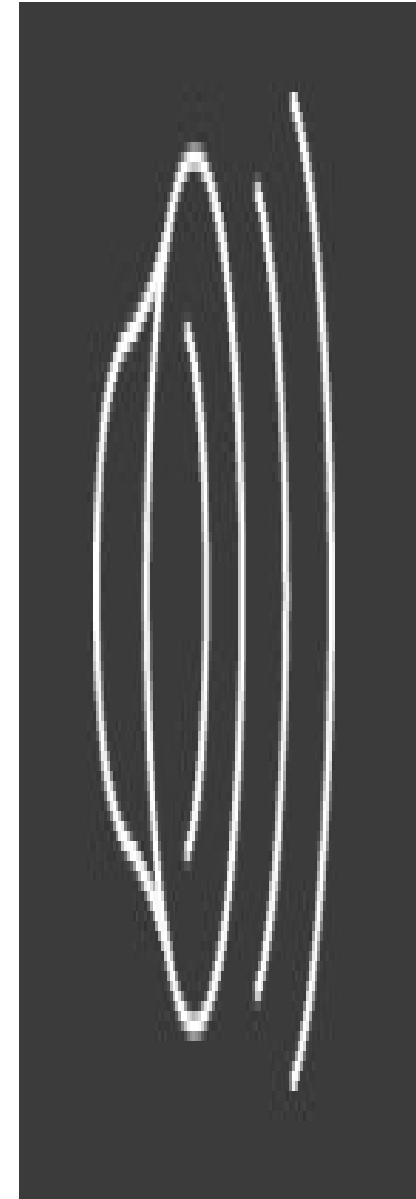
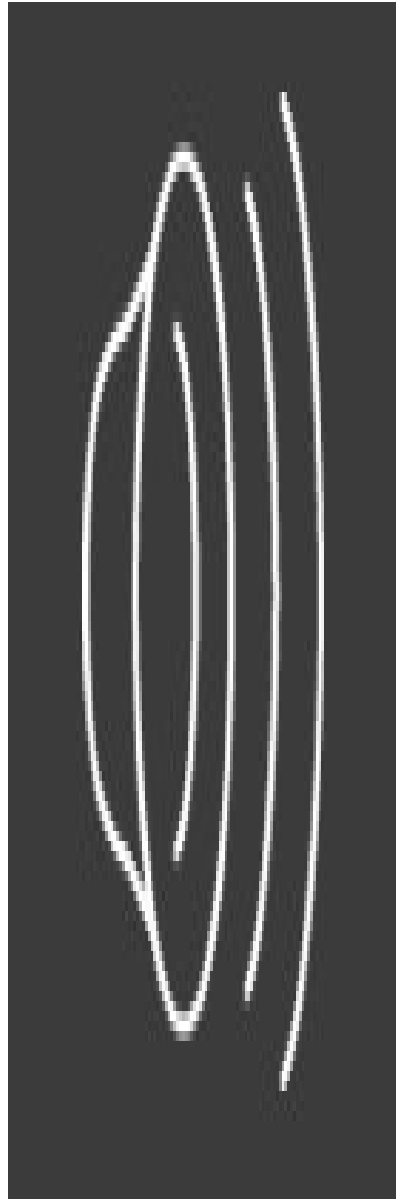
- Stable $m/n=0/1$ mode in the initial stage
- $m/n=1/1$ mode develops as the instability grows (kink or tearing instability) and reconnection occurs
- Tearing mode instability (slow evolution of the island/hot spot)
- Kink mode instability (sudden crash)
- Reconnection time scale is any different in these two types?



Sawtooth

- 2-D ECE imaging
- Firstly, (1,1) mode distorted. Then the combination of kink and local pressure driven instabilities leads to a small poloidally localized puncture in the magnetic surface at both the low and the high field sides of the poloidal plane.
- This observation closely resembles the “fingering event” of the ballooning mode model with the high- m mode only predicted at the low field side.

H.K. Park et al, PRL 96 195003 (2006)

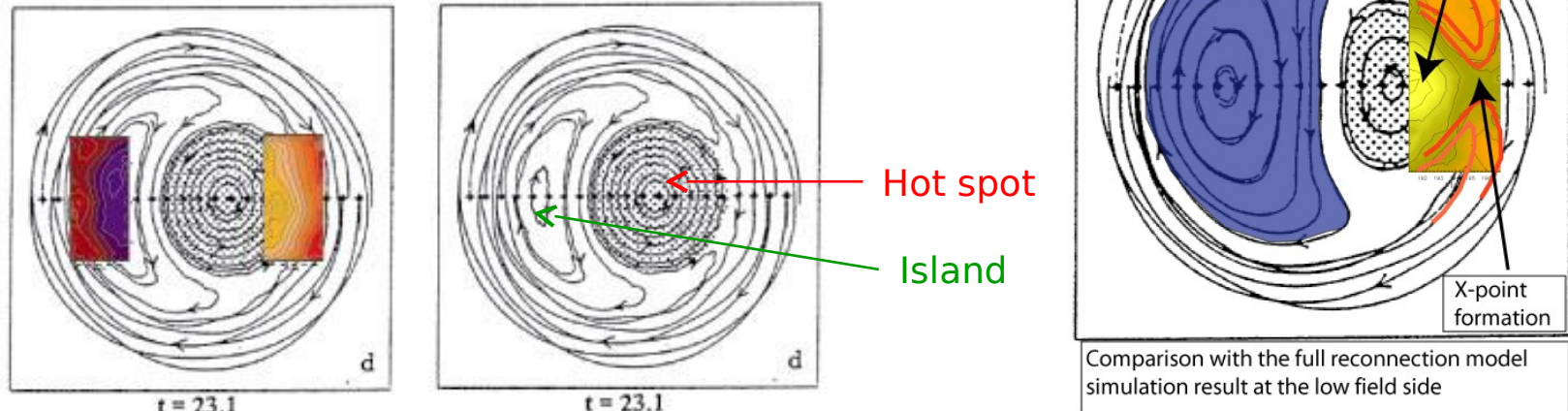


Sawtooth

- Comparison with theoretical models
 - The 2D ECE images are directly compared with the expected 2D patterns of the plasma pressure (or electron temperature) from various theoretical models.
 - The observed experimental 2D images are only partially in agreement with the expected patterns from each model:
 - a) The image of the initial reconnection process is similar to that of the ballooning mode model.
 - b) The intermediate and final stages of the reconnection process resemble those of the full reconnection model.
 - c) The time evolution of the images of the hot spot or island is partially consistent to those from the full reconnection model but is not consistent with those from the quasi-interchange model.

Sawtooth

- Comparison with the full reconnection model

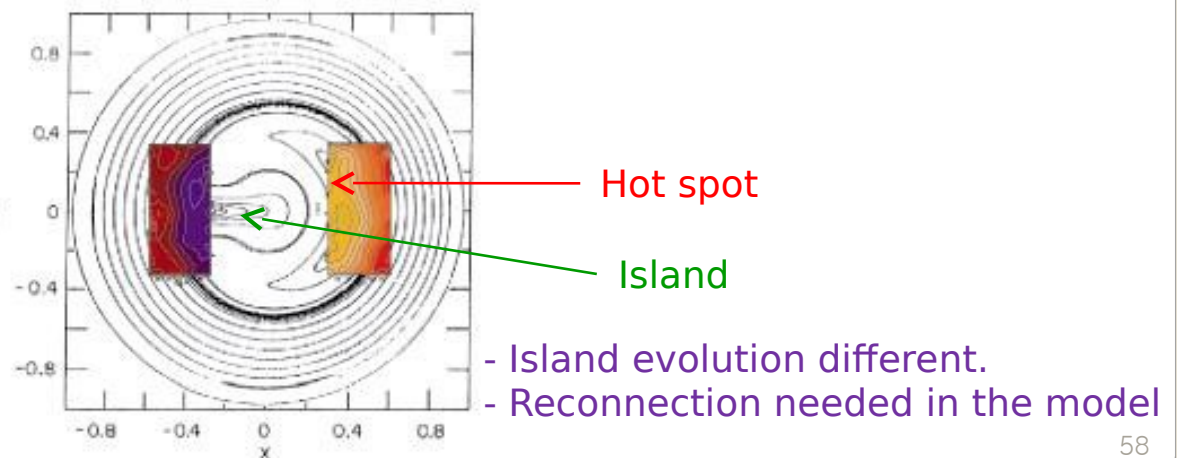
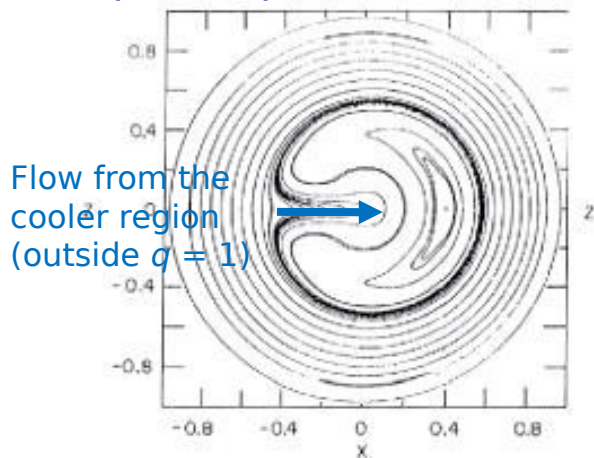


- The measurement and the simulation are strikingly similar.
- The shape of the hot spot is circular. It swells as it approaches the crash time, whereas the hot spot is shrinking as the island grows in the simulation.
- In the experimental result, there is no indication of a heat flow until the reconnection through the sharp temperature point takes place. In the full reconnection model, the formation of the island is the beginning of the reconnection process (heat flow), since it is assumed that the island is the result of a topological change of the magnetic field structure.
- It suggests a new physical mechanism which may delay the reconnection process (heat flow) until a critical time while the island grows to explain shorter collapse time in the experiment.

Sawtooth

- Comparison with the quasi-interchange model
 - The quasi-interchange model differs significantly from the full reconnection model and does not require any magnetic field reconnection process.
 - The core plasma having a flat q profile ($q \sim 1$) inside the inversion radius becomes unstable due to a slight change of the magnetic pitch angle (low shear).
 - In this model, there is no pressure driven instability. As the hot spot deforms into a crescent shape, the cooler outside portion of the plasma is convectively inducted into the core region, resulting in a flattening of the core pressure profile.
 - $q(0)$ requires ~ 1 .

J. A. Wesson, Plasma Phys. Controlled Fusion **28** 243 (1986)



Sawtooth

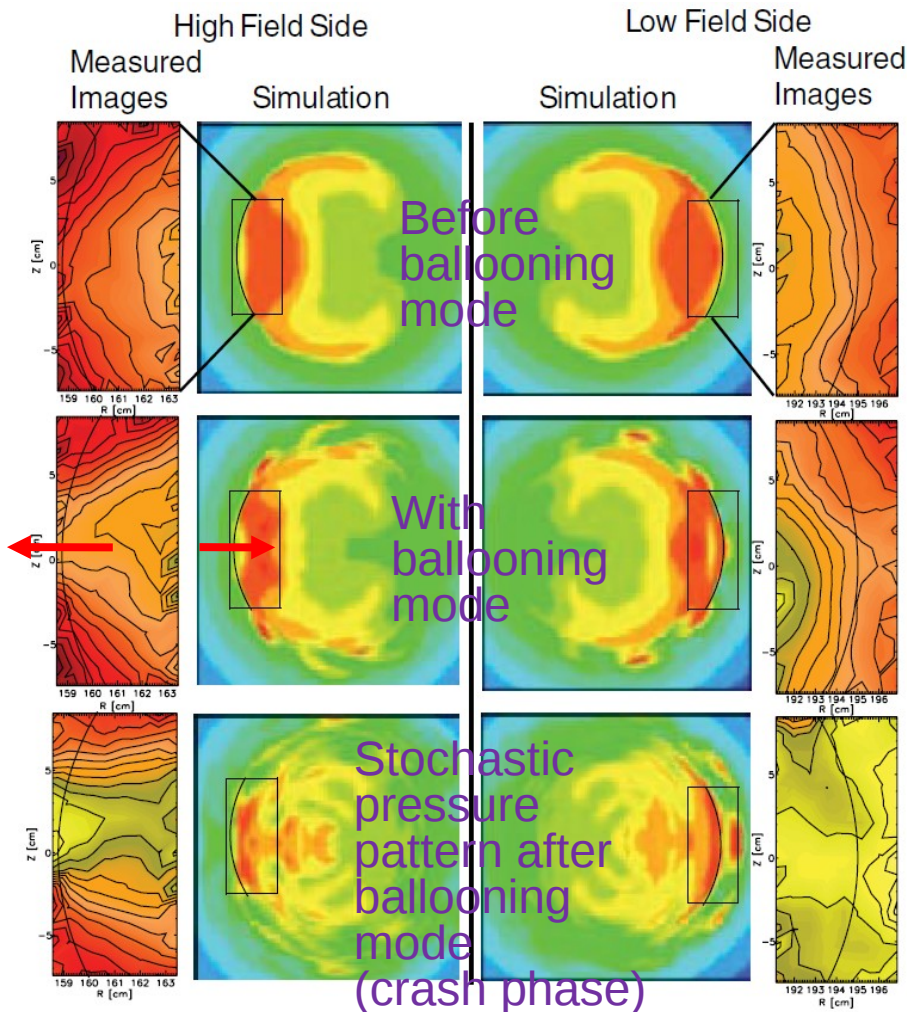
- Comparison with the ballooning mode model
 - Ballooning mode model has been introduced to account for the observed disruptions lead by a sawtooth crash in the high beta ($\beta_p \sim 1$ and $\beta_t(0) \sim 4\%$) plasmas in TFTR.
 - These modes are more pronounced at the bad curvature side of the magnetic surface (low field side of the torus).
 - It could be related to the sharp temperature point or “pressure finger” accompanied with the swelling of the $m/n=1/1$ mode at the low field side in experiments.
 - Dispersion of the heat is dominated by the global stochastic magnetic field in this model.
 - The magnitude of the pressure finger and the global stochasticity of the magnetic field are small at the moderate plasma beta.

*W. Park et al., Phys. Rev. Lett. **75** 1763 (1995)*

*Y. Nishimura et al., Phys. Plasmas **6** 4685 (1999)*

Sawtooth

- Comparison with the ballooning mode model



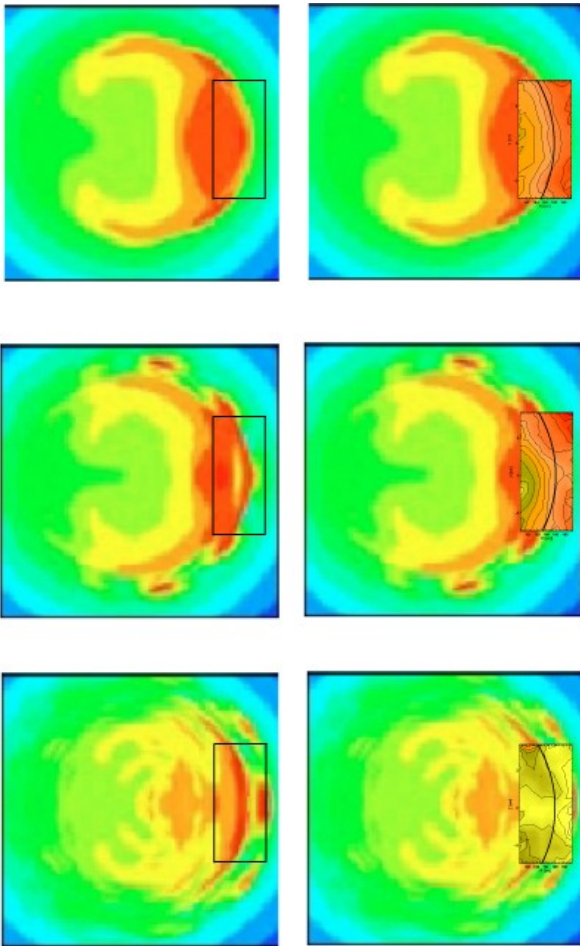
The pressure bulge with a smooth surface before the development of the ballooning mode is quite similar.

The sharp temperature point is strikingly similar.

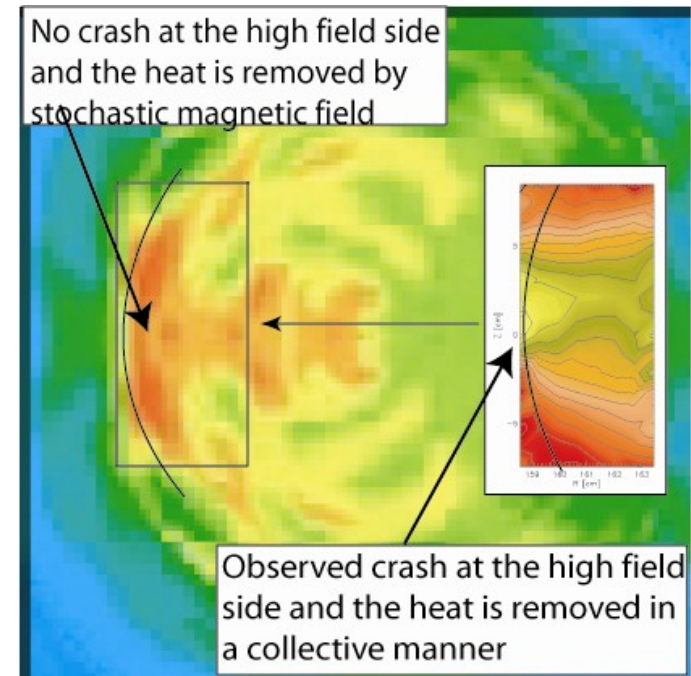
While the stochastic behavior is dominant in the pressure pattern of the simulation, the experimentally measured heat flow patterns are highly collective.

Sawtooth

- Comparison with the ballooning mode model



Low field side



Comparison with the Ballooning model simulation result at the high field side

Sawtooth

- Comparison with three theoretical models
- The time evolution of the hot spot and island partly resembles that of the full reconnection model, but it is not consistent with those of the quasi-interchange model.
- A pressure driven instability (sharp temperature point due to the distortion) of the $m/n=1/1$ mode accompanied with a kink instability or pressure bulge due to a finite pressure effect on the $m=1$ mode is consistent with the ballooning mode model, but the fact that the observed heat transport in the poloidal plane is well organized (collective behavior) suggests that the global stochasticity of the magnetic field line is not the dominant mechanism for this case.

References

- *R. Goldston and P. H. Rutherford, Ch. 20 in "Introduction to Plasma Physics", Institute of Physics Publishing, Bristol and Philadelphia, 1995*
- *Wolfgang Suttrop, "Experimental Results from Tokamaks", IPP Summer School, IPP Garching, September, 2001*